EXPERIMENTAL EVALUATION OF THE REACTOR CONTAINMENT SUMP

Beaver Valley Power Station Unit No. 2
Duquesne Light Company
Pittsburgh, Pennsylvania

by
Bruce J. Pennino
George E. Hecker

Sponsored by
Stone & Webster Engineering Corporation

ALDEN RESEARCH LABORATORY
WORCESTER POLYTECHNIC INSTITUTE

August 1983

EXPERIMENTAL EVALUATION OF THE REACTOR CONTAINMENT SUMP

Beaver Valley Power Station Unit No. 2
Duquesne Light Company
Pittsburgh, Pennsylvania

by
Bruce J. Pennino
George E. Heckez

Sponsored by
Stone & Webster Engineering Corporation

ALDEN RESEARCH LABORATORY
WORCESTER POLYTECHNIC INSTITUTE

August 1983

EXPERIMENTAL EVALUATION OF THE REACTOR CONTAINMENT SUMP

BEAVER VALLEY POWER STATION UNIT NO. 2
DUQUESNE LIGHT COMPANY
PITTSBURGH, PENNSYLVANIA

by

Bruce J. [illegible]nnino
George E. Hecker

Sponsored by
Stone & Webster Engineering Corporation

George E. Hecker, Director

ALDEN RESEARCH LABORATORY
WORCESTER POLYTECHNIC INSTITUTE
HOLDEN, MASSACHUSETTS

August 1983

ABSTRACT

Recirculation spray pumps withdraw water from the reactor containment sump after a postulated loss of coolant accident for re-injection into the core and containment building.

A 1:3 scale hydraulic model of the reactor containment sump for the Beaver Valley Power Station-Unit No. 2 was used to evaluate flow conditions and to develop methods which minimize swirl and vortex activity at the inlets to four recirculation spray pumps. A principal objective of the study was minimizing the reactor building water level for acceptable pump performance. To assure acceptable operation of the pumps, the model was tested for a wide range of possible approach flow distributions and water levels. The test program included testing of two and four pump operation combinations, and evaluation of 50 percent blockage of the vertical screens and/or racks located around the sump. The tests were designed to assure that no air-entraining vortices would form, that head losses across the screens and in the inlet would be acceptable, and that swirl in the pump suction pipes would be minimal. The test data included vortex severity, swirl angle, and inlet losses.

Without rack or screen blockage, testing with the original design indicated air-drawing vortices occurred at the four pump inlets with the reactor building water level at EL 694' and lower. At inlets A, C, and D, increasing the containment water level to EL 695'-6" (695.5') eliminated the air entraining vortices. However, undesirable flow patterns and vortices were not eliminated at inlet B until the water level reached the solid roof over the pump inlets at approximately EL 697'.

In order to eliminate the air entraining vortices and minimize the required reactor building water level, modifications to the sump were tested. The modifications found to be most effective included multiple layers of horizontal gratings in the sump and lowering the inlets. For the final design, the

inlet elevation for pumps A, C, and D was lowered from EL 691'-11 1/2" (691.96') to 691'-2 1/2" (691.21'). Inlet B, because of its proximity to a drainage trench outlet, was only lowered to EL 691'-6 1/2" (691.54') leaving it 5 1/2" (0.46') above the sump floor compared to the 1 1/2" (0.13') high lip at the other inlets.

Test results with the horizontal gratings and lowered inlets indicated that the minimum water level that permitted vortex free operation or no surface air bubble entrainment varied with the number of pumps operating and the location of blockage on the vertical screens or racks located around the sump. With the racks and screens free of obstructions, a containment water elevation of 693'-2 3/8" (693.2') was the minimum acceptable level for four pump operation with each inlet having a flow of 2570 gpm. Acceptable four pump operation with the worst case 50 percent screen blockage would require a containment level of EL 693'-9 1/2" (693.8'). A containment level of EL 693.6' was required with four pumps operating and the most severe case of 50 percent rack blockage.

For two pump operation, with the flow per pump equaling 3480 gpm, the most severe rack blockage produced a minimum acceptable containment water level of EL 693.5'. The most severe screen blockage for the two pump condition produced a minimum acceptable containment level of EL 693.8 ft.

The maximum velocities on the containment floor with four pumps operating and a containment level of EL 693.2' were generally less than 1.7 ft/sec.

TABLE OF CONTENTS

	Page No.
ABSTRACT	i
TABLE OF CONTENTS	iii
INTRODUCTION	1
DESCRIPTION OF PROTOTYPE	2
ADVERSE FLOW CONDITIONS TO BE INVESTIGATED	4
SIMILITUDE	6
Froude Scaling	8
Similarity of Vortex Motion	9
Dynamic Similarity of Flow Through Screens and Grates	12
MODEL DESCRIPTION	15
INSTRUMENTATION AND OBSERVATION TECHNIQUES	17
Flow Measurement	17
Pressure Gradelines	17
Pipe Swirl	18
Vortex Activity	19
Observation of Flow Patterns	19
Head losses Across Screens and Containment Level	19
TEST PROCEDURE	21
TEST RESULTS	22
Original Design	22
Effect of Farfield Flow Distribution	22
Effect of Flowrate	23
Effect of Water Level	24
Modified Design	25
Effect of Water Level	25
Gratings Over Inlets	26
Initial Blockage Tests	28
Final Design	29
Tests with "Before Switch Over" Flows	29
Final Blockage Tests	31
Inlet Loss Coefficients	33

TABLE OF CONTENTS (continued)

	Page No.
CONCLUSIONS	35
REFERENCES	38
FIGURES	
APPENDIX (Under Separate Cover)	
Laboratory Test Notes, Instrument Calibrations, and Calculations	

INTRODUCTION

The reactor containment building of the Beaver Valley Unit No. 2 generating station is provided with a containment depressurization system which includes the Reactor Containment Sump (RCS) and the recirculation spray pumps. The Recirculation Spray System (RSS) is designed to depressurize and cool the reactor core and reactor containment building in the event of a Loss of Coolant Accident (LOCA).

The Alden Research Laboratory (ARL) of Worcester Polytechnic Institute (WPI) was authorized by Stone & Webster Engineering Corporation to construct and test a model of the containment sump (ESSOW 2BVS-132). The objective of the study was to investigate any flow conditions in the sump that could adversely affect the performance of the recirculation spray system pumps in accordance with NRC Reg. Guide 1.82 (16). It was desirable to eliminate any air-entraining vortices while minimizing the operational level of the sump. Swirl in the approach to the pumps and inlet losses were evaluated since they can affect the available NPSH. During the study, various pump operating conditions, approach flow distributions, water levels, and grating and screen blockages, were tested in the model.

The model study included two test phases. During the first test phase, a minimum containment water level for a particular set of remedial design changes was determined based on a severe blockage condition at the racks and specified pump flows. During the second phase of testing at lower pump flows, a severe screen blockage condition was postulated and the sump design was modified so that acceptable inlet performance would result at water levels near the minimum values previously determined.

This report presents the major findings of both phases of this study and includes a description of the prototype, model, and recommended final design. The conditions investigated, similitude considerations, test procedures, instrumentation, and interpretation of results are also presented.

DESCRIPTION OF PROTOTYPE

The Reactor Containment Sump (RCS), together with four recirculation spray pumps, are part of the recirculation spray subsystem of the containment depressurization system. The reactor containment sump is located on the periphery of the reactor containment building as shown in Figure 1. A roof at approximately EL 697 ft (Figure 2) covers the pump sump, vertical racks, and screens. Vertical racks are located around the periphery of the roof and vertical double screens are located inside of the racks. The outside screen, Figure 2, has a 3/4 inch square opening while the inside screen has a 3/32 inch square opening. The sump is divided by a pair of racks with two screens between the racks, Figure 2. The screens have 3/32 inch square openings.

With the original design, the inlets for the recirculation spray pumps, four 12 inch diameter pipes, extended through the sump floor and terminated at EL 691'-11 1/2" (691.96'). Figure 2 shows details of the sump, screens, and pump inlets. After the inlet pipe passes through the sump floor it is embedded in concrete and each pipe supplies one pump. Figure 3 shows the lay-out of the RSS piping in the vicinity of the sump. As shown in Figure 1, in the vicinity of the sump there are various equipment, piping, and steel and concrete columns that would influence flow patterns approaching the sump. The floor of the reactor building generally slopes to the sump and has two levels separated by a 2 ft wide rectangular shaped trench, bottom approximately EL 691'-5" (691.42'), which enters the sump in the vicinity of inlet B. On the north side of the trench, Figure 1, the floor is approximately EL 692'-10" (692.83'). On the south side of the trench, the floor is approximately EL 691'9" (691.75'), and a vertical plate, designated the drainage dam, divides the sump (Figure 2). The transition between the two sump floor elevations occurs in the vicinity of the trench.

In the event of a LOCA, water from the Refueling Water Storage Tank (RWST) is sprayed inside the containment by means of the quench spray pumps (injection mode of the Emergency Core Cooling System (ECCS). The water is dispersed

through the containment structure, collects on the floor, and drains into the RCS. The recirculation spray pumps start after a time delay. In the recirculation spray mode, two pumps supply each spraying header and the flow is cooled by the recirculation coolers. When a low level is reached in the RWST, the flow from two spray pumps is automatically diverted to the low head safety injection pump discharge lines. The pumps can operate in various combinations "before switch over from recirculation spray mode", BSO, and "after switch over to injection mode", ASO. Figure 4 shows the various combinations and flowrates for 2, 3, and 4 pump combinations. In order to satisfy the minimum necessary heat removal requirements, the two pump combinations, either pumps A and C or pumps B and D, are the most critical operating condition, with each pump having a flow of 3480 gpm. With a low level in the containment building "before switch over", the expected pump flows for the four pump combination would be 2570 gpm/pump. The maximum flood level in the reactor building is approximately EL 708'-6" (708.5').

Initially testing was conducted with ASO flows shown in Figure 4. Thereafter, the ASO flow rates for pumps C and D were reduced approximately 450 gpm per pump. Therefore, the test flows for the initial phase of testing should be considered conservative.

ADVERSE FLOW CONDITIONS TO BE INVESTIGATED

The following are some of the likely flow conditions in a containment recirculation sump which could cause poor pump performance and, hence, were investigated during the model study.

1. Entrained Air - Air-entrainment in the suction pipes could be due to: air-entraining vortices existing in the sump; suction of entrapped air below top cover plates in a submerged sump; or other factors, such as breakflow jet impingement. An air concentration in the suction pipe of 3 to 5 percent, could lower the efficiency of the pump considerably. Hence, air-entrainment is recognized as a major flow condition in the sump to be examined and eliminated.

2. Swirling Flow - The various possible approach flow patterns, together with possible vortexing, could induce considerable swirl in the suction pipes, and, depending on its duration and intensity, could be undesirable for the pumps. Excessive swirl produces unsteady loading on the impeller, and also affects the intake and pipe friction losses, thereby affecting the available NPSH. The amount of allowable swirl varies with pump design and has not been firmly established. However, to be conservative, swirl should be minimized and 5 degrees or less is generally considered acceptable for extended periods of operation.

3. Losses Leading to Insufficient NPSH - A poorly designed sump could result in large intake losses. Intake losses caused by screens, poor entrance conditions, vortex suppression devices, etc., may add up to a value such that the required NPSH of the pump is not satisfied.

The most severe flow patterns, which can produce air-entrainment, swirling flow, and the greatest head losses, result during operation with a large portion of the racks or screen areas blocked. NRC criteria has established in Reg. Guide 1.82 that up to 50 percent of the racks or screen area could be

blocked by broken pieces of pipe insulation or other material. Therefore, rack and screen blockage tests are conducted to confirm the adequacy of the sump design for all expected conditions.

The model investigation of adverse flow conditions includes: the measurement of swirl using a swirl meter located in the suction pipes; the measurement of pressures and water levels to determine energy losses and loss coefficients; and the observation of vortices or other flow abnormalities.

SIMILITUDE

The study of dynamically similar fluid motions forms the basis for the design of models and the interpretation of experimental data. The basic concept of dynamic similarity may be stated as the requirement that two systems with geometrically similar boundaries have geometrically similar flow patterns at corresponding instants of time (1). Thus, all individual forces acting on corresponding fluid elements of mass must have the same ratios in the two systems.

The condition required for complete similitude may be developed from Newton's second law of motion:

$$F_i = F_p + F_g + F_v + F_t \qquad (1)$$

where

F_i = inertia force, defined as mass, M, times the acceleration, a
F_p = pressure force connected with or resulting from the motion
F_g = gravitational force
F_v = viscous force
F_t = force due to surface tension

Additional forces may be relevant under special circumstances, such as fluid compression, magnetic or Coriolis forces, but these had no influence on this study and were, therefore, not considered in the following development.

Two systems which are geometrically similar are dynamically similar if both satisfy the dimensionless form of the equation of motion. Equation (1) can be made dimensionless by dividing all the terms by F_i. Rewriting each of the forces of Equation (1) as:

$$F_p = \text{net pressure} \times \text{area} = \alpha_1 \, \Delta p \, L^2$$

F_g = specific weight x volume = $\alpha_2 \gamma L^3$

F_v = shear stress x area = $\alpha_3 \mu \Delta u/\Delta y$ x area = $\alpha_3 \mu u L$

F_t = surface tension x length = $\alpha_4 \sigma L$

F_i = density x volume x acceleration = $\alpha_5 \rho L^3 u^2/L = \alpha_5 \rho u^2 L^2$

where

α_1, α_2, etc. = proportionality factors
L = representative linear dimension
p = net pressure
γ = specific weight
μ = dynamic viscosity
σ = surface tension
ρ = density
u = representative velocity

Substituting the above terms in Equation (1) and making it dimensionless by dividing by the inertial force, F_i, we obtain

$$\frac{\alpha_1}{\alpha_5} E^2 + \frac{\alpha_2}{\alpha_5} F^2 + \frac{\alpha_3}{\alpha_5} R^1 + \frac{\alpha_4}{\alpha_5} W^2 = 1 \qquad (2)$$

where

$E = \frac{u}{\sqrt{\Delta p/\rho}}$ = Euler number; $\frac{\text{Inertia Force}}{\text{Pressure Force}}$

$F = \frac{u}{\sqrt{gL}}$ = Froude number; $\frac{\text{Inertia Force}}{\text{Gravity Force}}$

$R = \frac{u L}{\mu/\rho}$ = Reynolds number; $\frac{\text{Inertia Force}}{\text{Viscous Force}}$

$$W = \frac{u}{\sqrt{\sigma/\rho L}} = \text{Weber number; } \frac{\text{Inertia Force}}{\text{Surface Tension Force}}$$

Since the proportionality factors, α_i, are the same in model and prototype, complete dynamic similarity is achieved if all the dimensionless groups, E, F, R, and W, have the same values in model and prototype. In practice, this is difficult to achieve. For example, to have the values of F and R the same requires either a 1:1 "model" or a fluid of very low kinematic viscosity in the reduced scale model. Hence, the accepted approach is to select the predominant forces and design the model according to the appropriate dimensionless group. The influence of the other forces would be secondary and are called scale effects (1, 2).

Froude Scaling

Models involving a free surface are constructed and operated using Froude similarity since the flow process is controlled by gravity and inertia forces. The Froude number, representing the ratio of inertia to gravitational force,

$$F = u/\sqrt{gs} \qquad (3)$$

where

u = average velocity in the pipe
g = gravitational acceleration
s = submergence, the representative linear dimension

was, therefore, made equal in model and prototype.

$$F_r = F_m/F_p = 1 \qquad (4)$$

In modeling of an intake sump to study the formation of vortices, it is important to select a reasonably large geometric scale to achieve large

Reynolds numbers and to reproduce the curved flow pattern in the vicinity of the intake (3). At sufficiently high Reynolds number, an asymptotic behavior of energy loss coefficients with Reynolds number is usually observed (2). Hence, with $F_r = 1$, the basic Froudian scaling criterion, the Euler numbers, E, will be equal in model and prototype. This implies that flow patterns and loss coefficients are equal in model and prototype at sufficiently high Reynolds numbers. A geometric scale of $L_r = L_m/L_p = 1/3.0$ was chosen for the model, where L refers to length. From Equations (3) and (4), using $s_r = L_r$, the velocity, discharge, and time (t) scales were:

$$u_r = L_r^{0.5} = 1/\sqrt{3.0} = 1/1.73 \tag{5}$$

$$Q_r = L_r^{2}\, u_r + L_r^{2.5} = 1/(3.0)^{2.5} = 1/15.6 \tag{6}$$

$$t_r = L_r^{0.5} = 1/\sqrt{3.0} = 1/1.73 \tag{7}$$

Similarity of Vortex Motion

Fluid motions involving vortex formation in sumps of low head pump intakes have been studied by several investigators (3, 4, 5, 6).

Viscous and surface tension forces could influence the formation and strength of vortices (4, 5). The relative magnitude of these forces on the fluid inertia force is reflected in the Reynolds and Weber numbers, respectively, which are defined as:

$$R = u\, d/\nu \tag{8}$$

$$W = \frac{u}{(\sigma/\rho r)^{1/2}} \tag{9}$$

where r = characteristic radius of vortex and d = intake diameter. It was important for this study to ascertain any deviations in similitude attributable to viscous and surface tension forces in the interpretation of model results. For large R and W, the effects of viscous and surface tension are minimal, i.e., inertial forces predominate. Surface tension effects are negligible when r is large, which will be true for weak vortices where the free surface is essentially flat. Conversely, only strong air core vortices are subject to surface tension scale effects. Moreover, an investigation using liquids of the same viscosity but different surface tension coefficients (σ = 4.9 x 10^3 lb/ft to 1.6 x 10^3 lb/ft) showed practically no effect of surface tension forces on the vortex flow (4). The vortex severity, S, is therefore mainly a function of the Froude number, but could also be influenced by the Reynolds number.

$$S = S\ (F,\ R) \tag{10}$$

Anwar (3) has shown by principles of dimensional analysis that the dynamic similarity of fluid motion in an intake is governed by the dimensionless parameters given by

$$\frac{4Q}{u_\theta\ d^2}\ ,\quad \frac{u}{\sqrt{2gs}}\ ,\quad \frac{Q}{\nu\ s}\ ,\quad \text{and}\quad \frac{d}{2s}$$

where

- Q = discharge through the outlet
- u_θ = tangential velocity at a radius equal to that of outlet pipe
- d = diameter of the outlet pipe

Surface tension effects were neglected in his analysis, being negligible for weak vortices. The influence of viscous effects was defined by the parameter $Q/(\nu\ s)$, known as a radial Reynolds number, R_R.

For similarity between the dimensions of a vortex of strengths up to and including a narrow air-core type, it has been shown that the influence of viscous forces becomes very small if $Q/(\nu\ s)$ is greater than 3×10^4 (3). As strong air-core type vortices, if present in the model, would have to be eliminated by modified sump design, the main concern for interpretation of prototype performance based on the model performance would be on the similarity of weaker vortices, such as surface dimples and dye-cores. In the model, R_R was approximately 5×10^4 for the range of conditions tested. Thus, viscous forces would have only a secondary role in the present study. This conclusion is also supported by Padmanabhan and Hecker (17) where various scale sumps were tested over a range of water levels and water temperatures. Dynamic similarity is obtained by equalizing the parameters $4Q/u_\theta d^2$, $u/\sqrt{2gs}$, and $d/2s$ in model and prototype. A Froudian model would satisfy this condition.

To compensate for any possible excessive viscous energy dissipation and consequently less intense model vortex, various investigators have proposed increasing the model flow and, therefore, the approach and intake velocity, since the submergence is maintained constant. Operating the model at the prototype inlet velocity (pipe velocity) is believed by some researchers to achieve the desired results (4). This is often referred to as the "Equal Velocity Rule", and is considered to give conservative predictions of prototype performance. The test program for this study included selective tests at prototype pipe velocities to determine if the test results exhibited any sensitivity to Reynolds number.

Since this study meets and exceeds the Reynolds number criteria, and all other non-dimensional parameters are equal in the model and prototype, no scale effects are expected in the final design.

At low water levels, the "Equal Velocity Rule" can produce excessive head loss and incorrect flow patterns. Areas of critical depth can occur in a model, but not be representative of prototype conditions. Therefore, the depth at

which the "Equal Velocity Rule" is applicable depends on the geometry of each model. This and other factors relevant to similitude of vortices are discussed in more detail by Hecker (14).

Dynamic Similarity of Flow Through Screens and Grates

In addition to providing protection from debris, screens and racks tend to suppress non-uniformities of the approach flow. The aspects of flow through screens and racks of concern in a model study are: (1) energy loss; (2) modification of velocity profile and the deflection of streamlines; and (3) production of turbulence. As all these factors could affect vortex formation in a sump, a proper modeling of screen and rack parameters is important.

In the prototype, sharp edged rectangular bars will be used to construct the racks and the area blocked by the bars (solidity) will be approximately 16 percent. Similarly shaped bars were used in the model with a solidity of 29 percent. Analysis indicated that under normal conditions the prototype head loss would be a negligible 0.01 ft. In the model, with a somewhat lower Reynolds number and greater solidity, the head losses would be slightly higher, but still negligible. The model racks had more horizontal members, and fewer vertical members than the prototype. This could, to small extent, influence the flow distribution and swirl passing through the racks. However, in any case, 50 percent blockage would produce the greatest change in velocity distribution and head loss, far outweighing any small effects due to the differences in rack details.

The loss of energy (pressure drop) across a screen dictates the effectiveness of the screen in altering velocity profiles. The pressure drop across the screen is analogous to the drag induced by a row of cylinders in a flow field and could be expressed in terms of a pressure-drop coefficient K (or alternately a drag coefficient), defined as (7),

$$K = \frac{\Delta p}{1/2\ \rho\ U^2} = \frac{\Delta H}{U^2/2g} \qquad (11)$$

where

Δp = drop in pressure across the screen

U = mean velocity of approach flow

ρ = density of the fluid

ΔH = head across the screen

g = acceleration due to gravity

From the available literature on the topic (7, 8, 9), it may be seen that

$$K = f(R_s, S', \text{Pattern}) \qquad (12)$$

where

R_s = screen Reynolds number, $U\ d_w/\nu$, d_w being the wire diameter

S' = solidity ratio, equal to the ratio of closed area to total area of screen

Pattern = geometry of the wire screen

If the solidity ratio and the wire mesh pattern are the same in the model and prototype screens, the corresponding values of K would only be a function of the screen Reynolds number. This is analogous to the coefficient of drag in the case of the circular cylinder. It is known that K becomes practically independent of R_s at values of R_s greater than about 150 (10, 11). However, for models with low approach flow velocity and with fine wire screens, it is necessary to ascertain the influence of R_s on K for both the model and prototype screens before selecting screens for the model which are to scale changes in velocity distribution.

Velocity modification equations relating the upstream velocity profile and downstream velocity profile have been derived based on different theories (7).

Most of these indicate a linear relationship between upstream velocity profile, and downstream velocity profile, shape and solidity ratio of screen, and value of K. If the wire shape and solidity ratios are the same in the model and prototype screens, it is possible to select a suitable wire diameter to keep the values of K approximately the same for the model and prototype screens at the corresponding Reynolds number ranges. Identical velocity modifications would be produced by the respective screens if the loss coefficients were identical.

For the prototype screens, no. 6 wire cloth d_w = 0.063 inches, and no. 1 wire mesh d_w = 0.192 inches will be used and R_s exceeded 150. In the model using the same screens as the prototype and no blockage, the minimum velocity occurs with the sump level at EL 697 ft. For this condition, R_s > 150 at the no. 1 mesh and was approximately 50 at the no. 6 wire cloth. With R_s of 50, the model would have approximately 25 percent greater head loss than the prototype. Since the vast majority of all tests were conducted at near minimum levels that reduced the effective screen area to 50 percent or less of the area at EL 697 ft, and many tests were conducted with only half of that area with simulated blockage, it was concluded that R_s was sufficiently great in the model to meet similitude criteria.

MODEL DESCRIPTION

The model was constructed to a geometric scale of 1:3.0 with boundaries, as indicated in Figure 1.

The model was constructed within an existing elevated tank that provided a maximum containment level of EL 701 ft. This maximum level in the model was selected, compared to the maximum prototype level of EL 708'-6" (708.5'), because the strength of vortex activity diminishes with increasing depth, and a sufficient depth would be available over the inlets to show this trend by EL 701 ft.

Model boundaries were chosen at locations where flow pattern control in the prototype would be sufficiently removed from the sumps to avoid boundary effects, especially once screen blockage is considered. The flow distributor along the model boundary could be easily modified so that the farfield flow distribution could be a variable during testing. Figure 5 shows an overall view of the model with the flow distributor along the right border. The cooling coils, Figure 5, are in the middle of the figure, and the associated head loss was approximated with wire mesh. Since screen blockage has consistently generated the most severe vortices and swirl in the numerous past sump studies at ARL, it was unnecessary to precisely model the details of the cooling coils.

The roof over the sump was modeled with acrylic for viewing purposes, and the depths of the roof beams were scaled since they inhibit swirling motion when they contact the water surface. Racks, columns, screens, major piping, and equipment were simulated, and Figure 6 shows details of columns in the vicinity of the sump, and figure 7 shows the original pump inlets.

The pump inlet piping was modeled with 4 inch smooth acrylic pipe. A length of approximately 20 diameters downstream of the inlets was provided in pump lines A and D, which had ten dual pressure taps at 1 diameter intervals for

measuring pressure gradients. The pipe elbows were modeled with smooth radius steel elbows. Pump lines B and C each had one set of pressure taps for comparison of data with lines A and D. Pumps B and C had an access port (Figure 8) for installing the vortimeter, and Figure 9 shows the vortimeter. Figure 3 shows the limit of prototype piping that was modeled, and Figure 10 shows the pressure taps located on pump line D.

A centrifugal pump recirculated water from the Laboratory sump to upstream of the flow distributor. Valves in each pump line controlled the flow and the maximum flow capability of each line exceeded that required to simulate the maximum prototype inlet velocity of 10.9 ft/sec. ASME orifice flow meters (12) were provided in each line to measure the flow, and it is estimated they had an accuracy of approximately ± 3-5 percent.

The equipment and pipes in the vicinity of the sump were constructed basically of wood in accordance with the simulated overall dimensions. Model screens were the same as the prototype screens. The coarse screen was no. 1 wire mesh with 0.192 inch wire diameter, and the fine mesh was no. 6 with 0.063 inch wire diameter.

INSTRUMENTATION AND OBSERVATION TECHNIQUES

Flow Measurement

Flowrates were measured by ASME standard orifice meters and air-water manometers for differential pressure measurement.

Pressure Gradelines

The pressure gradelines in inlet lines A and D were measured by pairs of piezometers at ten locations (Figure 10) using a 1 psi differential pressure (DP) cell, using the reactor building water level as the reference pressure. Figure 2 shows the location of the floor tap for the containment building water level. It should be noted that the building water level was measured upstream of the screens and grates around the sump area, Figure 2. The pressure gradeline for the straight pipe was extrapolated to the inlet entrance, and the area average velocity was used to calculate the pipe velocity head which was added to the extrapolated pressure gradeline. The extrapolated total head at the pipe entrance was subtracted from the reactor building water elevation to determine the total inlet loss. Since the screens, gratings, and one elbow in pump line A and two elbows in pump line B, produce energy losses, the difference between the extrapolated total head and the reactor building level includes these losses. Pipe friction losses must be added to determine prototype head loss. An entrance loss coefficient was calculated by

$$K_T = \frac{\Delta H_T}{\frac{U^2}{2g}} \qquad (13)$$

where

K_T = total loss coefficient = $K_G + K_s + K_i + K_E$
ΔH_T = total head loss, ft
K_G = grating loss coefficient
K_s = screen loss coefficient

K_i = inlet loss coefficient
K_E = elbow(s) loss coefficient

Figure 11 shows the procedure for determining K_T. In the final design where horizontal gratings were used to minimize vortex activity, the loss produced has been included in K_T.

The differential pressure cell was calibrated in place using two variable height columns of water (stilling wells) and a vernier point gage that could be read to 0.001 ft. Tubes from the stilling wells connected to the DP cell. For a difference in water level between the wells, a voltage was observed on a voltmeter. With this data, a straight line calibration curve of differential pressure versus volts could be plotted. For each head loss test the calibration curve was checked and a least square fit of the data was obtained. All of the pressure taps on the pipes were manifolded to the DP cell for rapid data acquisition. As an overall check, a limited amount of pressure head data in the pump lines and across the screens was recorded using the point gage and stilling wells.

Pipe Swirl

Average swirl in the suction pipes was measured by a cross vaned swirl (vortimeter) meter shown in Figure 9. Studies at ARL (13) have shown that a swirl meter with vane diameter 75 percent that of the the pipe diameter best approximates the solid body rotation of the flow. The rate of rotation of the vortimeter was determined by counting the number of blades passing a fixed point over a time interval of two minutes.

An average swirl angle, θ, was defined as the arc tangent of the maximum tangential velocity divided by the axial velocity. It is generally conservatively considered that θ should be less than 5 degrees. The maximum tangential velocity is the rotational speed times the circumference of the pipe, π d N, and the average swirl angle is defined by:

$$\theta = \arctan\left(\frac{\pi d N}{U}\right) \qquad (14)$$

where

N = revolutions per second

d = pipe diameter, ft

U = mean axial velocity, ft/sec

Vortex Activity

Vortex activity was recorded by observing vortex strength on a scale from 1 to 6 (see Figure 12). Vortex strength was identified by using dye injection or addition of small floating "trash" consisting of wood chips. Generally, with consideration given to the model Reynolds number and other factors, vortex severity at a pump inlet should not continuously exceed type 3, but brief periods of type 4 may be considered acceptable. Since, as discussed herein under Adverse Flow Conditions to be Investigated, air ingestion due to any phenomena is of concern, the flow in the transparent pipe downstream of the inlets was observed. Flow conditions at an inlet were considered acceptable when the flow in the line was virtually free of air bubbles.

Observations of Flow Patterns

Visual aids, such as dye, were used to observe flow patterns. Photographic documentation was taken whenever appropriate. Velocities along the floor of the reactor building and at the gratings were measured with a miniature velocity meter calibrated at ARL in a towing tank.

Head Loss Across Screens and Containment Level

Head losses across the vertical racks and screens were measured using a point gage and stilling well system. Depending on the blockage arrangement at the racks or screens, the water level downstream of the vertical screens could vary because of the head loss that occurred at the double screen that divided

the sump. Figure 2 shows the location of sump floor taps, designated S1 and S2, that were used to measure the water level in the sump on each side of the double screens dividing the sump.

During the first phase of testing, a staff gage located on the north face of the column adjacent to the accumulator tank, Figure 1, was used to determine reactor floor water levels. During the second phase of testing, it was determined that at approximately EL 693'-6" (693.5') the staff gage located on the column indicated a containment level approximately 0.1' lower than was generally present in the containment due to the gage's location in an eddy produced by the column. At containment levels lower than EL 693'6" (693.5') the difference in reading between the staff gage and the general reactor water level increased because of increasing velocities. At higher water levels, the difference rapidly diminished. A staff gage located on the accumulator tank and the point gage system connected to a piezometric opening, shown in Figures 1 and 2, were used to measure levels during the 2nd phase of testing.

TEST PROCEDURE

Tests were conducted at the normal laboratory water temperature of approximately 55°F. The model was filled to the level specified for the test, and all piezometer and manometer lines were purged of air and zero flow differentials checked. During the first phase of testing, tests were conducted over the range of levels between EL 701 and approximately EL 693'6" (693.5'). As the study progressed, testing was predominantly conducted at levels below EL 695-694 ft. The required flowrates, in accordance with Figure 4, were then set and allowed to stabilize. The water level was checked and adjustments made if required, and flowrates were rechecked and readjusted, if necessary. With the majority of the tests conducted at levels below the elevation of the roof over the sump, the roof was removed in order to better observe vortices, inject dye, or insert small wood chips. Calibration curves for the differential pressure cell were performed as necessary as discussed under Pressure Gradelines. Vortex activity, swirl, or head loss data were recorded in accordance with the test order. The procedures used during data acquisition are discussed under Instrumentation and Observation Techniques. Swirl was observed in pump lines B and C, and pressure gradients were measured in pump lines A and D. A set of pressure taps were installed in pump lines B and D so that the pressure change (drop) to these taps could be compared with data recorded in the other two pipelines. Blockage tests were conducted using pieces of plywood to block portions of the gratings and/or screens and the personnel barrier indicated in Figure 1.

TEST RESULTS

Original Design

Effect of Farfield Flow Distribution

The purpose of this phase of testing was to determine the farfield flow distribution (Figure 13) that produced the strongest vortex activity at the inlets. Since the strongest vortices occur at relatively low levels, the approach flow pattern tests were conducted with the level in the containment at or above EL 694'. Above EL 694', the flow patterns did not change substantially. As discussed later, at lower levels the flow pattern on the floor varied because of the difference in floor elevations in the containment building.

In the model, the open area of the flow distributor was divided into thirds and the inflow proportioned to each area. Table 1 shows the three distributions evaluated.

TABLE 1

Farfield Flow Distributions

	Percent of Total Flow		
Distribution	Left	Center	Right
1	50	25	25
2	25	50	25
3	25	25	50

As found in other studies at ARL, testing indicated that the flow pattern and vortex severity at the inlets were not greatly affected by varying the farfield flow distribution. The overall flow pattern in the containment building and sump produced by distribution 2 is shown in Figure 13, and Figure 14 shows

the mean and maximum vortices observed at the four inlets with distributions 1 and 2. Test results with distribution 3 were similar to those observed with distributions 1 and 2. The data in Figure 14 indicates that the mean vortex activity, i.e., the average vortex observed over the test, did not differ substantially with farfield flow distribution, but the maximum observed vortices were somewhat greater with distribution 1. Therefore, during the remainder of the test program, flow distribution 1 was used. It should be noted in Figure 14 that air drawing vortices to the inlet, type 6, Figure 12, occurred continuously at pump B, and the maximum vortices at pump D were type 4, trash pulling. The type 4 vortex strength is defined using small pieces of floating trash as an indicator in the model. The actual presence of trash in the prototype inlet area is not really a concern because of the screens.

The effect of the farfield flow distribution on vortices was generally determined at water level EL 695'-6" because, as discussed later, at lower water levels the vortices with the original design were continuously so severe that no differentiation with distribution could be determined.

Effect of Flow Rate

As discussed under Similitude, the "Equal Velocity Rule" is proposed by some as a conservative technique for overcoming scale effects in modeling vortex formation. However, studies have indicated that a minimum inlet Reynolds number is a more fundamental basis for judging scale effects (see Similitude section). In "Equal Velocity" tests, the same flow patterns as in the prototype, will occur as long as head losses are small and relatively the same over the model area. If head losses become significant, such as could occur during blockage tests and low level tests, false data and conclusions can result. In the extreme, critical depth can occur in a model, with resulting flow restriction and re-distribution which would not occur in the prototype. Such was the case when levels in the reactor building were less than approximately EL 694 ft. Therefore, prototype velocity tests were not conducted below EL 694 ft.

In the prototype with a flow of 3480 gpm at inlets A and B, the corresponding inlet velocity would be 9.87 ft/sec. At inlets C and D with a flow of 3160 gpm, the prototype inlet velocity would be 8.96 ft/sec. The corresponding (Froude scaled) model flows which produced these inlet velocities in the model, as shown in Figure 15, would be 6029 and 5474 gpm. Dividing the equal velocity flow by the normal Froude scaled flow indicates there was a 73 percent increase in model flow for the equal velocity tests.

As indicated in Figure 15, with the water level EL 695'-6" (695.5'), the increased flowrate typically increased the mean vortex activity to some extent, but there was no fundamental change in test results. For type 4 vortices or lower, the vortices observed increased by approximately one increment. It was concluded that above EL 694, selected prototype velocity tests would be conducted to evaluate any alternative designs. Below EL 694, because of areas of critical depth on the reactor building floor, only Froude scaled tests would be conducted. For the data in Figure 15, as indicated by Figure 4 for four pumps operating, a flow of 3480 gpm at inlets A and B, and 3160 gpm at inlets C and D would occur "after switch over".

Effect of Water Level

Test results with the original inlet design, Figure 2, indicated that without blockage the angle of swirl was usually 5 degrees or less, and never exceeded approximately 6 degrees. The ingestion of air was a much more significant problem than the swirl angle. The original inlets could not be operated at steady state with a level of EL 693 in the reactor building because of large entrainment of air. At EL 694, all four inlets had continuous type 6 vortices and the air entrainment was visually quite large, Figure 10. As the water level increased, the vortex activity decreased, and Figure 16 shows the effect of water level on the maximum vortices at the pumps with the original inlet design. Inlets A, C, and D could operate without air entraining vortices with the containment water level EL 695'-6" (695.5') or greater. At EL 697, just prior to the water level touching the roof, the maximum vortices at all inlets

without any screen blockage were type 3 or less. Not considering blockage, but requiring that no air entrainment occur at any of the inlets, the minimum level for operation was approximately EL 697'. Because the objective was to minimize the water level for vortex free operation, blockage tests were not conducted since the level for vortex free operation was too great and blockage would normally further increase the required water level with the original design.

Figure 17 shows a summary of mean vortex severity with the original design. After the water level touched or exceeded the roof over the inlets, vortex activity was eliminated and the swirl was less than 5 degrees. Therefore, no further testing was conducted at levels exceeding the roof elevation.

Modified Design

Effect of Water Level

Generally, the greater the submergence of an inlet, the less susceptible it is to surface vortex formation. As a means of increasing submergence, the top elevation of inlets A, C, and D was reduced approximately 9 inches to EL 691 ft 2 1/2 inches, leaving approximately 1 1/2 inch between the inlet elevation and the sump floor. At this time in the test program, inlet B was not lowered because of its proximity to the drainage trench which would cause the inlet to be routinely filled with water.

At containment water levels below approximately EL 694'-6" (694.5'), as indicated in Figure 18, the lowered inlets operated with the time averaged mean vortex activity lower than with the original inlets. The lowered inlets could operate to approximately water EL 693'-6" (693.5') without experiencing air entraining vortices. At levels exceeding approximately EL 694'6" (694.5'), the mean vortex activity was somewhat increased with the lowered inlets. The increase in the mean vortex activity was due to vortices increasing at inlet C from type 1 to type 3 when the inlet was lowered; thereby the

combined average of the three inlets (Figure 18) was increased. Presumably, the flow pattern changed sufficiently around inlet C to increase the mean vortex strength, but the maximum vortex did not exceed type 3, as shown in Figure 19 where the maximum observed vortices are shown as a function of water level. At inlets A and D, the vortex activity was reduced to some extent with the lowered inlets. A comparison of Figures 16 and 19 indicates the beneficial effect of lowering the A and C inlets. With the lowered inlets, pumps A and C could be operated without entraining air to EL 694. At inlet D, the maximum vortices were not reduced, but on the mean vortex severity was reduced.

In summary, without blockage, the lowering of inlets A, C, and D was beneficial and permitted the operation of pumps A and C to EL 694 without entraining air, and the mean vortex activity was reduced at inlet D. Inlet D would require a minimum containment level of approximately EL 695; and inlet B, which was not lowered, would require a minimum level of approximately 695.5'. It was concluded that the desired minimum operating level would be obtained with the inlets lowered.

Gratings Over Inlets

In order to minimize air entrainment at inlets B and D, and minimize the operational water level allowing for blockage, horizontal gratings were installed in the sump over the inlets. Initially, small areas of gratings over the inlets were considered, but observations indicated that the vortex core could enter the inlet without passing through the grating as the flow patterns changed with blockage. A substantial reduction of vortex severity and lower water levels was obtained with the grating cage shown in Figure 20. Placing the cage over an inlet eliminated vortex activity and minimized the water level at which vortices occurred. However, the covering of the entire sump area with grating has the advantage of dissipating angular momentum wherever it may try to form. Therefore, gratings over the entire sump area

were evaluated, and Figure 21 shows horizontal gratings located over the sump area.

The horizontal gratings were effective in minimizing vortex activity. Testing indicated that one level of grating was insufficient at higher water levels and with blockage. With two levels of gratings, the mean vortex activity at Froude scaled velocity was approximately type 2 with the water level at EL 694 ft and 693 ft 6 inches (Figure 22). As the sump level increased, the vortex activity increased as the larger mass of water over the inlets started rotating. The vortex activity was type 3 or less except at inlet B which had vortex activity greater than type 3 for 3 percent of the time for levels between EL 696 ft and EL 693 ft 6 inches. Because of the somewhat stronger vortices at inlet B, a third level of grating over this inlet was evaluated. Figure 23 shows details of the three levels of gratings shown in Figure 21. As discussed later, blockage tests required modifications to the intermediate design shown in Figure 23.

With prototype inlet velocities, Figure 22, the mean vortex activity was approximately type 3 or less and the swirl angle at all inlets was 3 degrees or less with two levels of gratings. The maximum vortex at all inlets did not exceed type 4. As was observed with the original design (Figure 15), the large increase in velocity (flow) did not produce greatly different vortex severity.

With the horizontal gratings in place, the benefit of lowering the inlets below their original elevations was confirmed at Froude scale velocities with the test results shown in Figure 24. With the level in the reactor containment building at EL 694 ft, the data in Figure 24 indicates that vortex activity was less severe with the lowered inlets, for which the mean vortex was approximately type 2. At inlets A, C, and D with the original inlets and horizontal gratings, the vortices were approximately type 3 or greater. The lower graph in Figure 24 indicates that at original inlet D, type 4 vortices occurred approximately 60 percent of the time, while at inlets A and C, type 4

vortices occurred approximately 25 percent of the time with the gratings. These data indicate that the lowered inlets are preferred even with the multiple layers of gratings.

Initial Blockage Tests

Using the modified sump design, blockage tests were conducted to determine the effect on vortex activity. Experience has shown that the most severe vortex activity occurs when up to 50 percent of the area of the vertical racks or screens is blocked. The more severe vortex activity with blockage is due to adverse flow patterns that increase the strength of rotational flows; and at low levels, the increased head loss across the screens reduces the submergence on the inlets. Figure 25 shows some of the blockages that were evaluated with various combinations of pumps and the water level EL 694 ft in the reactor building. The effect of blockage was generally evaluated over a range of containment levels, but the most severe cases were found to be at EL 694 and lower. In all cases, the trench screen was assumed blocked because of its low elevation.

For each case in Figure 25, the pumps operating are indicated along with the maximum observed vortex. No air entrainment, type 5 or 6 vortices, was observed during the testing and generally the maximum observed vortex was type 2 with occasional type 3 or 4 vortices. For the "after switch over flows" (ASO) and cases shown in Figure 25, the rack blockage shown in Figure 25(f) was initially determined to be the most severe case. The vortex data in Figure 26 indicates that the vortices were typically type 2 between EL 696.0 to approximately EL 693.5'. Air entrainment began when the containment building water level dropped below approximately EL 693.5'.

Additional testing at approximately EL 693.6' indicated that the level within the sump with the ASO flows was sensitive to leakage through the blockage, and that the initial staff gage, because of its location in an eddy, indicated a containment level approximately 0.1 ft lower than a more representative level

indicated by a gage in a revised location. Furthermore, somewhat greater head losses could be generated by another arrangement of screen blockage compared to the rack blockage of Figure 25f. For the ASO flows, Figure 26 shows the mean vortices recorded. Tests with the worst screen blockage are discussed under "Final Design."

Final Design

Tests with "Before Switch Over" Flows

Since a worse screen blockage compared to rack blockage case was determined, and at the lowest containment water level the "before switch over" (BSO) flows (Figure 4) would occur, additional testing was conducted to determine the minimum containment water building level for no blockage and the worst blockage cases.For four pump operation, the "before switch over" (BSO) flow per inlet would be 2570 gpm.

For the two pump combination, the BSO flow per inlet would be 3480 gpm and either pumps B and D or A and C would operate. Since the minimum flow required to effect the necessary heat removal would occur with the two pump case, two pump operation was the most critical.

Because head losses were predominantly at the screens, the water level within the sump varies with the number of pumps operating, their flows, the percentage of blocked screen or rack area, the distribution of blockage, and the containment water level. Since the location of blockage for either the two or four pump combinations may force the operating pumps to be supplied through the double screen that divides the sumps, a significant head loss can occur across this set of screens. In order to determine the effect of the reduction of inlet flows (four pump operation) to the BSO flow, vortex and head loss tests were conducted initially without blockage.

Head loss data from the reactor to the sump with four pump operation and no blockage is shown in Figure 27 for the sump with grating details shown in Figure 23. For inlet flows of 2570 gpm, the pumps could operate to a containment water level of approximately EL 693.1 ft with occasional air bubbles seen in the inlet B pipe. The small amount of air observed at inlet B was not due to vortex entrainment, but attributed to a "nappe" forming at the screen due to the relatively large head loss at the screen and the low water level in the sump. This nappe entrained some air, which was then pulled into inlet B.

In order to minimize air entrainment, inlet B was lowered 5 inches to EL 591'-6 1/2" (691.54'). An additional level of grating was attached to the level 1 grating over inlet B, Figure 28, and air entrainment was eliminated. It was determined that without blockage and a flow of 2570 gpm per pump, the minimum acceptable containment water level for four pumps was EL 693.2 ft. By comparison, as seen in Figure 27, with a flow of 3480 gpm, inlet B had a continuous large air inflow at EL 693.1 ft. Lowering inlet B 5 inches, reducing the flow, and adding a double grating over inlet B permitted the sump to operate to a containment water level of EL 693.2 ft. The additional level of grating over inlet B was attached below the previous grating and the bars were aligned. In order to obtain the best performance of the horizontal grating, the direction of the level 2 grating should be parallel to the front screens, while the bars at level 1 and 3 are perpendicular to the direction of the level 2 bars. Figure 29 shows the final gratings over inlets B and D.

Generally, at low containment and, therefore, sump water levels, the swirl angle increased as the sump level dropped. Figure 30 indicates that a swirl angle of approximately 9 degrees was measured at inlet B when the sump level was approximately EL 692.9 ft, which is the approximate elevation of the bottom of the level 2 grating. From the head loss data in Figure 27, this sump level would correspond to approximately EL 693.2 ft in the containment. The data in Figure 30 indicates the swirl angle decreased as the sump level increased above the level 2 grating. This was also true at the other inlet with a swirl meter. Except at extreme low levels when the sump water level

was close to the grating 2 level, the swirl angle was 5 degrees or less. Since the amount of allowable swirl at a pump impeller is not well defined, brief periods of swirl above 5 degrees would not be detrimental to pump performance and this was agreed to by Stone and Webster.

Final Blockage Tests

Testing indicated that the minimum acceptable containment level varied with two or four pump operation and the location of blockage. For four pump operation with an inlet flow per pump of 2570 gpm, Figure 31 shows the most severe blockage at the rack, Figure 31(b), and at the screen, Figure 31(c). For comparison purposes, the levels in the containment building and on both sides of the divider screens are given along with data for the no blockage case, Figure 31(a). No leakage was present at the screens or rack, and the containment water level was measured at the revised staff gage, Figure 1, and with the point gage system.

Figure 31 indicates that the minimum acceptable containment level would be EL 693.8 ft and EL 693.6 ft for the most severe screen and rack blockages, respectively. Vortices were type 3 or less, and for both blockage cases, the minimum containment level was determined by the nappe at the screen adjacent to inlet B entraining air bubbles and the occasional withdrawal of an air bubble from the water surface in the sump. The levels on both sides of the sump, indicated by S1 and S2, were equal in the rack blockage case. With screen blockage, Figure 31 (c), the level at inlets B and D was approximately 0.4 ft lower than at inlets A and C due to the head loss across the double divider screen. In general, somewhat lower acceptable containment water levels would result if the screen losses were reduced. Figure 32 shows the rapid change in head loss that occurred with the worst rack blockage, Figure 31(b), as the containment level decreased. With the containment at EL 693.6 ft, the effect of blockage is indicated by the head loss increasing from 0.1 ft to approximately 0.7 ft. Figure 33 shows the variation of head loss during four-pump operation with the worst screen blockage case, Figure 31(c), as the

containment level varies. Above a containment water level of EL 694, the losses become relatively small. Below this level, the losses rapidly increased for inlets B and D with more loss occurring at the double divider screen that at the blocked screen.

The likelihood of screen blockage versus rack blockage depends on the type of insulation used in the reactor containment building. If a major portion of the insulation is of the reflective metallic type, studies indicate (15) that the material will settle on the reactor floor and not be carried to the racks unless velocities on the floor exceed 2 ft/sec. If carried to the racks, it could not reach or block the screens. Figure 34 shows velocities measured on the containment floor with four pump operation and a containment water level of EL 693.2. The data indicates that floor velocities are generally less than 1.7 ft/sec. As the containment level increases, these velocities diminish.

With only two pumps operating and a flow of 3480 gpm per pump, the minimum acceptable containment level was also determined by the blockage that produced a nappe at the screen adjacent to inlet B. The nappe would entrain air and inlet B would, on occasion, withdraw an air bubble from the water surface. However, no significant vortices were observed at inlet B. For two pump operation with 50 percent blockage, the vortices were type 2 or less for all cases. Figure 35(a) shows that the minimum acceptable operating level in the containment building was EL 693.8 ft with the screen blockage arranged so that considerable flow to pumps B and D was supplied through the double divider screen. As indicated in Figure 35(a), the head loss across the blocked screen was only 0.1 ft while the loss across the divider screen was 0.7 ft, producing a sump level of EL 693.0 ft at inlets B and D. Figure 36 indicates the large reduction of head loss that occurs with the worst blockage as the containment level increases. With the containment at approximately EL 694 ft, the total loss has dropped to approximately 0.3 ft. When pumps A and C operated with the worst screen blockage condition at the same containment water level, no vortices were observed. No worse screen blockage condition could be determined for inlets A and C.

The worst grating blockage for inlets B and D is shown in Figure 35(c), and the minimum containment level was EL 693.5'. Figure 35(d) indicates that inlets A and C would operate at this level without air drawing vortices for the worst grating blockage, and no worse blockage arrangement could be determined for these inlets.

In using the above described minimum acceptable reactor water levels, it should be realized that the exact acceptable level varies with the percent blockage and whether or not some water may leak through the blocked area. As shown by the data on Figures 32 and 33, the head loss across the rack and screens varies dramatically with the reactor water level, and similarly, data not shown indicates that the head loss at a given minimum water level varied considerably with the percent and manner of placement of the model boards simulating the insulation debris.

Inlet Loss Coefficients

Inlet loss coefficients were determined with the modified design as shown in Figure 23 in accordance with procedures discussed under Instrumentation and Observation Techniques.

Inlet loss coefficients were determined from pressure gradients measured along inlet pipes A and D without screen or rack blockage and the containment level EL 695.0 and greater. The data from these lines were compared with data from a single tap located on each of lines C and D and indicated that loss coefficients for all inlets were approximately equal. The inlet loss coefficients exclude friction but include all upstream gratings and screens, horizontal and vertical, the inlet loss, and one or two elbows, depending on the inlet pipe. In order to calculate hydraulic gradelines for the worst blockage cases, the sump level on the appropriate side of the divider screens should be used. This calculation would be slightly conservative since K_T includes the small screen loss that occurred without blockage. For inlet D with two elbows included, the original inlet loss coefficient was approximately 0.83. With

the additional horizontal gratings and the lowering of the inlet, K_T increased to approximately 0.97. At inlet A with one elbow included, K_T with the original inlet was approximately 0.63 and increased to 0.77 with the final gratings and lowered inlet. With the assumption that flow patterns and inlet losses were approximately equal at inlets A and D, the difference between K_T at inlets D and A, 0.83 and 0.63, respectively, would be the loss coefficient for one elbow. On this basis, the loss coefficient for each elbow is approximately 0.20, which agrees with literature values of approximately 0.15.

CONCLUSIONS

Original Design

Testing with the original design indicated continuous air entraining vortices at all of the inlets at low water levels in the reactor containment building. Without consideration of blockage, the original inlet design required that the water level in the reactor containment building exceed EL 695.5 ft for no air entrainment to occur at inlets A, C, and D. At inlet B a containment water level of approximately EL 697.0 ft was required.

Modified Design

The following modifications were made to the sump in order to improve performance and achieve a lower minimum acceptable water level.

1. The top elevations of inlets A, C, and D were lowered 9 inches.

2. Two levels of 1-1/2 inch horizontal grating were placed over inlets A, C, and D while three levels were placed over inlet B (Figure 23). The third upper level grating was required to minimize swirl at higher water levels.

These modifications were sufficient to eliminate vortex activity over inlets A, C, and D. Inlet B, however, still produced vortices at lower sump water elevations.

Final Design

In addition to the previous sump modifications, the final design modifications (Figure 28) consisted of lowering inlet B 5 inches and installing an additional grating above inlet B at the lowest level resulting in a double thickness (3 inches) at that level. This arrangement proved satisfactory in suppressing

vortices at all containment water levels above the minimum determined, as discussed below.

At containment levels below approximately EL 693.75 ft, the head losses across the vertical screens and sump divider doubled screens became relatively large with blockage of the vertical screens or racks. A loss of 0.5' or greater could occur depending on the blockage location. Operation with blockage of 50 percent of the racks or screens established the minimum acceptable water level in the reactor containment building.

For four pump operation with the flow per pump equalling 2570 gpm, the minimum acceptable containment level was EL 693.2 ft without any blockage, Figure 35. With the worst screen or grating blockage, the minimum acceptable levels were EL 693.8 and EL 693.6 ft, respectively. For two pump operation with blockage, the minimum containment level was EL 693.8 ft and EL 693.5 ft with screen and grating blockage respectively. These test results are summarized in Table 2, below.

TABLE 2

Minimum Acceptable Water Level in Reactor Containment Building

Final Design

Condition	Pump Flow gpm	Pumps Operating	Minimum Acceptable Level in Containment Building EL (ft)
No Blockage	2570	A,B,C,D	693.2
Grating Blockage	2570	A,B,C,D	693.6
Screen Blockage	2570	A,B,C,D	693.8
Grating Blockage	3480	B and D or A and C	693.5
Screen Blockage	3480	B and D or A and C	693.8

The swirl angle at the inlets was generally less than 5 degrees. At minimum containment water levels, the maximum swirl angle had values up to approximately 9 degrees. However, test data indicates that this is a transient case and the swirl angle diminishes rapidly with increased water levels and above EL 694 the swirl angle was less than 5 degrees. It was agreed upon with Stone and Webster that this would not be considered in violation of the 5 degree maximum swirl angle as specified in the ESSOW.

Velocities were measured on the floor of the containment building with four pumps operating (no blockage) and the containment level EL 693.2 ft. This data indicated that velocities were generally less than 1.7 ft/sec.

The addition of horizontal gratings over the inlets and lowering the inlets A, C, and D increased the entrance loss coefficient by approximately 0.14. With the final design, the total inlet loss coefficient for inlet A was 0.77, and at inlet D with two elbows included, the loss coefficient was approximately 0.97. These inlet loss coefficients do not include screen and rack losses during blockage with debris.

REFERENCES

1. Rouse, H., Handbook of Hydraulics, John Wiley & Sons, 1950.

2. Daily, J.W., and Harleman, D.R.F., Fluid Dynamics, Addison-Wesley Publishing Company, 1965.

3. Anwar, H.O., Weller, J.A., and Amphlet, M.B., "Similarity of Free-Vortex at Horizontal Intake," Journal of Hydraulic Research, IAHR 16, No. 2, 1978.

4. Daggett, L.L., and Keulegan, G.H., "Similitude Conditions in Free Surface Vortex Formations," Journal of Hydraulics Division, ASCE, Vol. 100, pp. 1565-1581, November 1974.

5. Hattersley, R.T., "Hydraulic Design of Pump Intakes," Journal of the Hydraulics Division, ASCE, pp. 233-249, March 1965.

6. Reddy, Y.R., and Pickford, J., "Vortex Suppression in Stilling Pond Overflow," Journal of Hydraulics Division, ASCE, pp. 1685-1697, November 1974.

7. Baines, W.D., and Peterson, E.G., "An Investigation of Flow Through Screens," Trans. ASME, pp. 467-477, July 1951.

8. Papworth, M., "The Effect of Screens on Flow Characteristics," British Hydromechanics Research Association, Report TN1198, November 1972.

9. Weighardt, K.E.G., "On the Resistance of Screens," The Aeronautical Quarterly, Vol. IV, February 1953.

10. Padmanabhan, M., and Vigander, S., "Pressure Drop Due to Flow Through Fine Mesh Screens," Journal of the Hydraulics Division, ASCE, HY8, August 1978.

11. Tennessee Valley Authority, "Flow Through Screens," Report No. 87-8, May 1976.

12. ASME, Fluid Meters, Their Theory and Application, edited by H.S. Bean, 6th Edition, New York, NY, 1971.

13. Durgin, W.W., and Lee, H.L., "The Performance of Cross-Vane Swirl Meters," ASME Winter Annual Meeting, 1980.

14. Hecker, G.E., "Model-Prototype Comparison of Free Surface Vortices," ASCE Journal of the Hydraulics Division, Vol. 107, No. HY10, October 1981, p. 1243.

15. Brocard, D.N., "Buoyancy, Transport, and Head Loss of Fibrous Reactor Insulation," NUREG/CR-2982, Alden Research Laboratory, Holden, MA, November 1982.

16. Nuclear Regulatory Commission Regulatory Guide 1.82, Sumps for Emergency Core Cooling and Containment Spray Systems, June 1974.

17. Padmanabhan, M., and Hecker, G.E., "Assessment of Scale Effects on Vortexing, Swirl, and Inlet Losses," ARL Report 48A, September 1982.

FIGURES

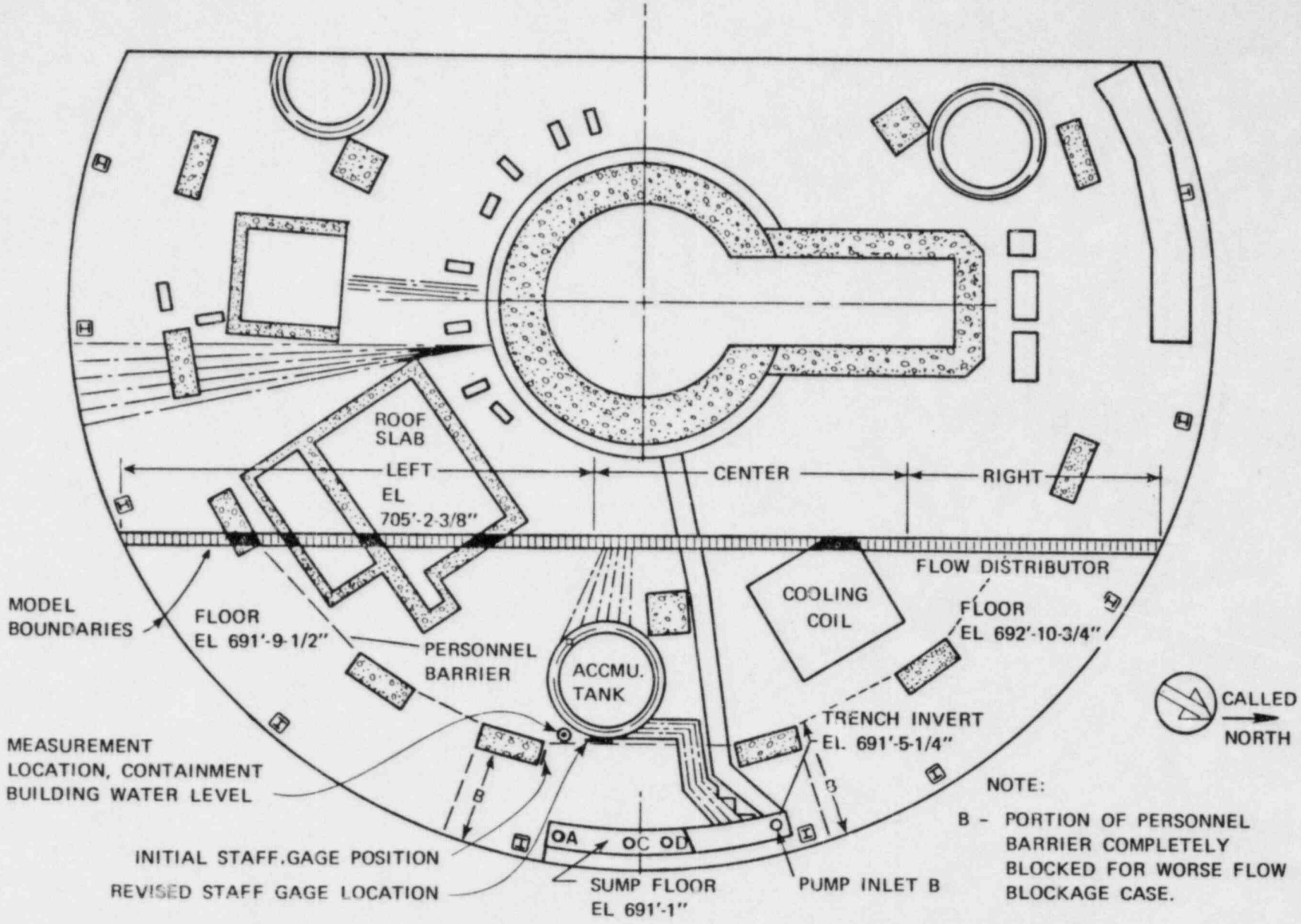

FIGURE 1 OVERALL DETAILS AND MODEL BOUNDARY REACTOR CONTAINMENT BUILDING AND SUMP

ARL

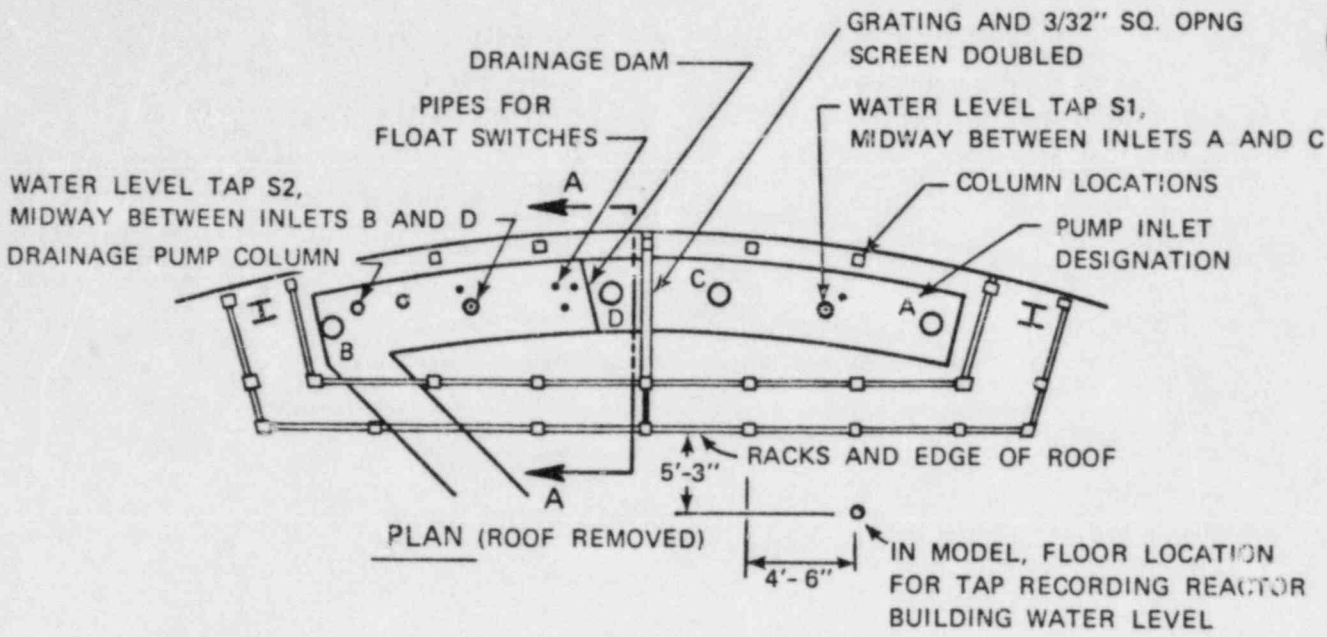

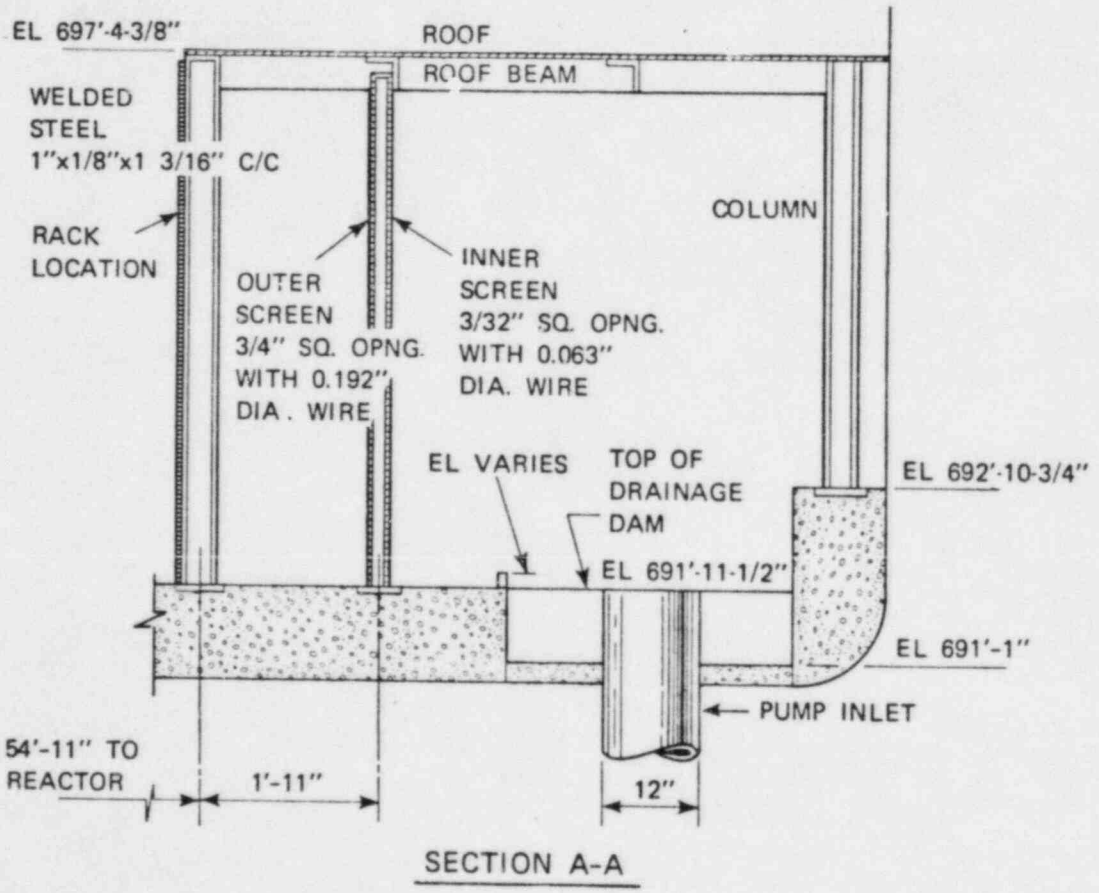

FIGURE 2 ORIGINAL SUMP DETAILS

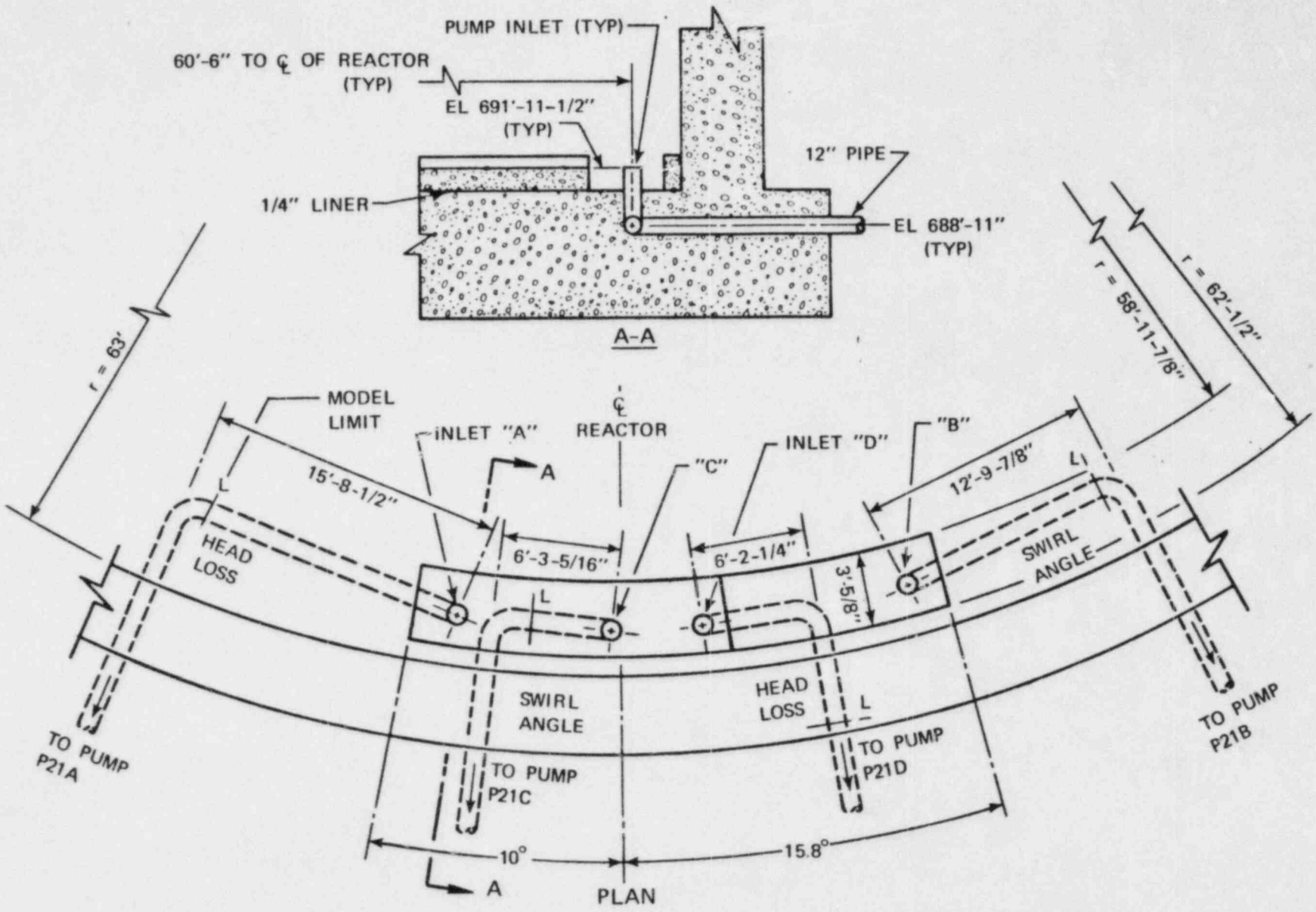

FIGURE 3 ORIGINAL RECIRCULATION SPRAY PIPING AND INLETS

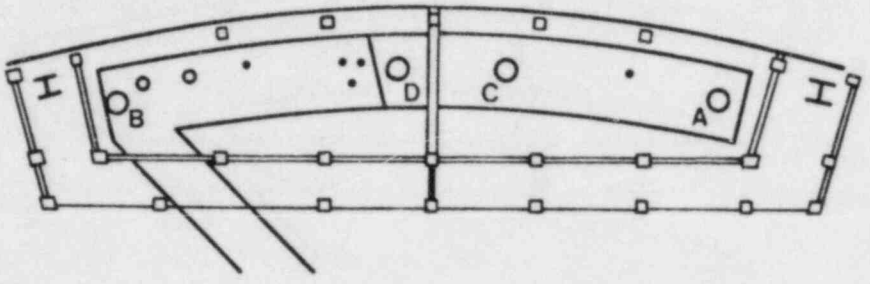

PROTOTYPE FLOW RATES

Pump* #	FLOW RATE PER PUMP (GPM)													
	2 Pump Combination				3 Pump Combination								4 Pump Combination	
	A and C		B and D		A,B, and C		B,C, and D		C,D, and A		A,B, and D		A,B,C, and D	
	BSO	ASO	BSO	ASO	BSO	ASO	BSO	ASO	BSO	ASO	BSO	ASO	BSO	ASO
P21A	3480	3480			3480	3480			2570	3480	2570	3480	2570	3480
P21B			3480	3480	2570	3480	2570	3480			3480	3480	2570	3480
P21C	3480	3850			2570	3850	2570	3160	3480	3160			2570	3160
P21D			3480	3850			3480	3160	2570	3160	2570	3850	2570	3160

BSO = Before Switch Over from Recirculation Spray Mode

ASO = After Switch Over to Injection Mode for Recirculation Spray Pumps (Recirculation Mode of the ECCS)

*Designated by letter only in text

FIGURE 4 PUMP OPERATION COMBINATIONS AND FLOWS

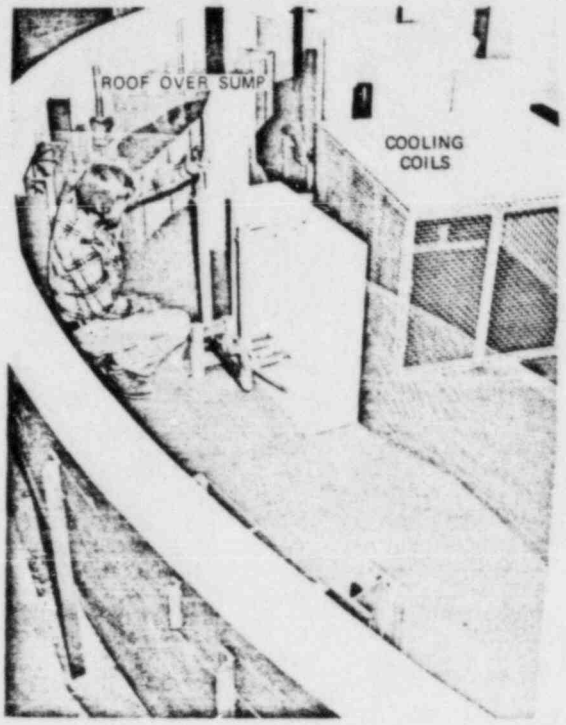

FIGURE 5 OVERALL VIEW OF MODEL

FIGURE 6 SUMP DURING CONSTRUCTION

ARL

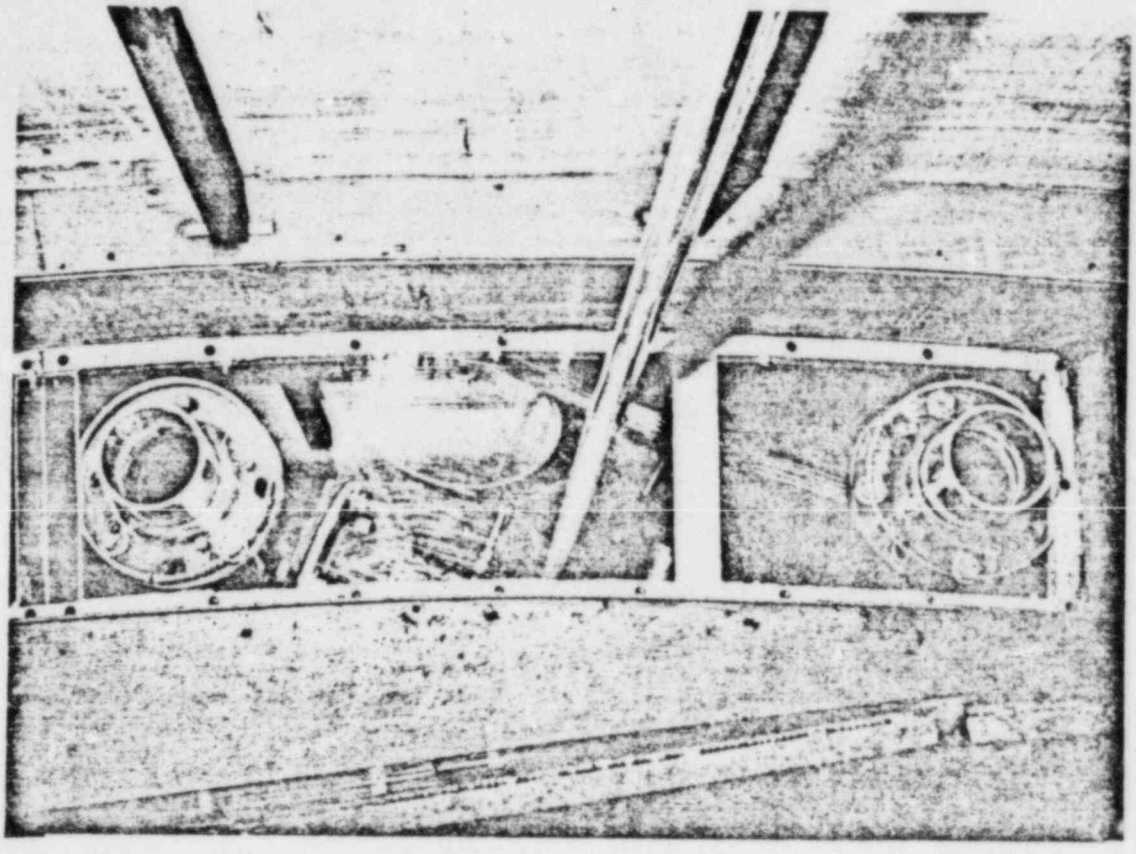

FIGURE 7 ORIGINAL PUMP INLETS

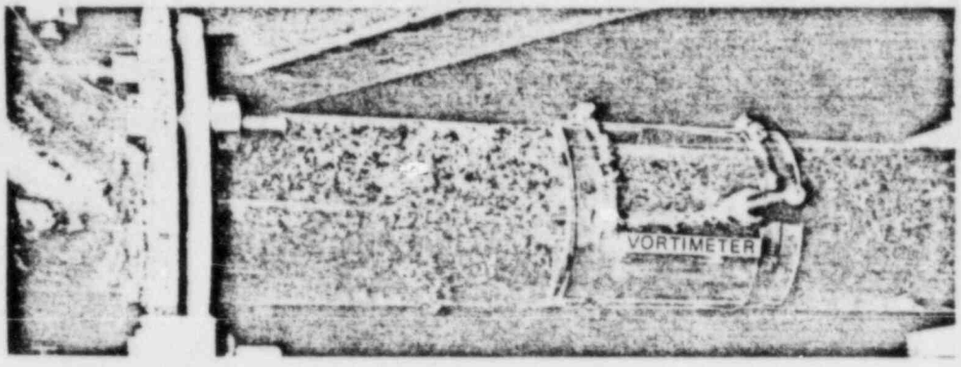

FIGURE 8 VORTIMETER ACCESS PORT

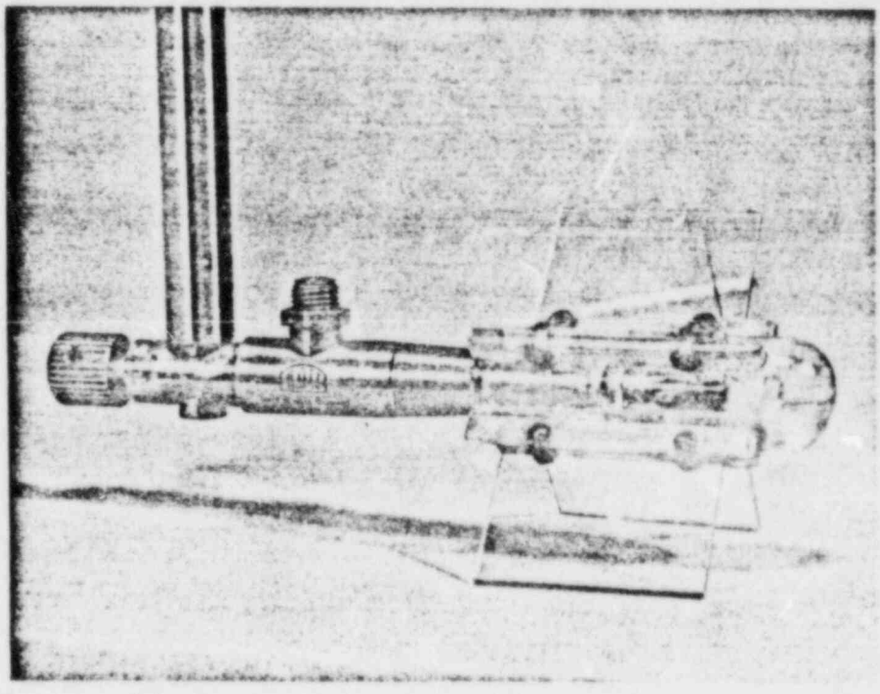

FIGURE 9 VORTIMETER

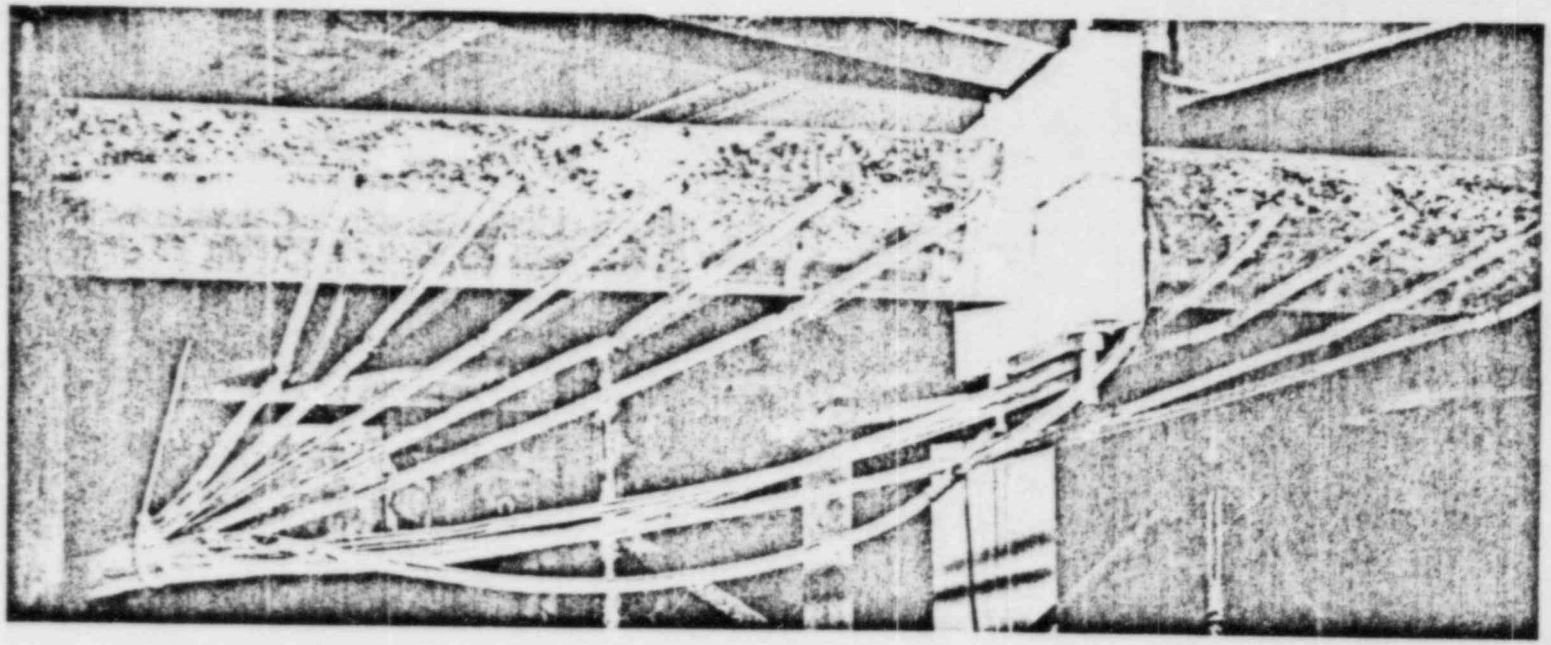

FIGURE 10 PRESSURE TAPS ON PUMP LINE AND AIR INGESTION FOR ORIGINAL DESIGN

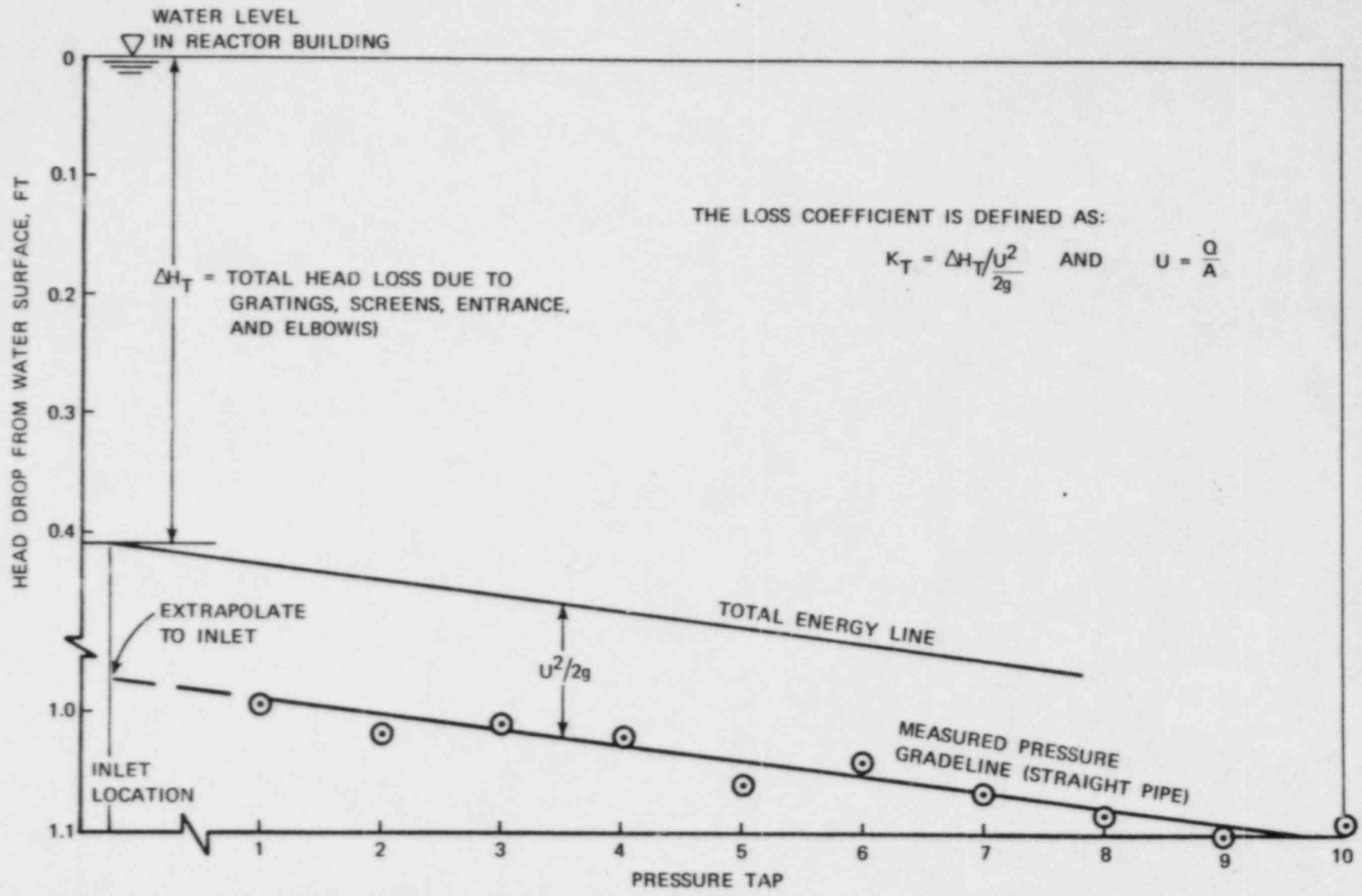

FIGURE 11 DEFINITION OF INLET LOSS COEFFICIENT

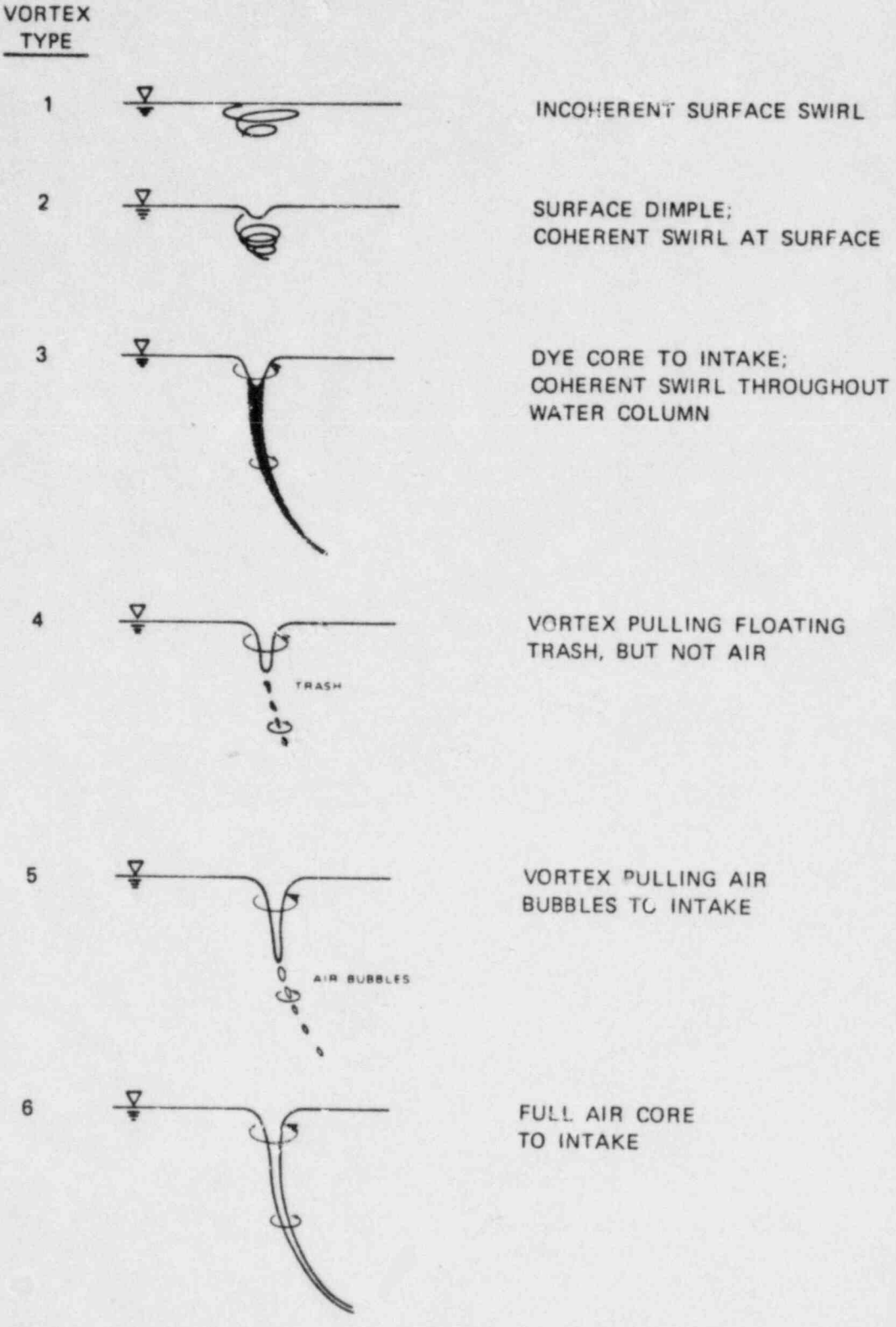

FIGURE 12 CLASSIFICATION OF FREE SURFACE VORTICES

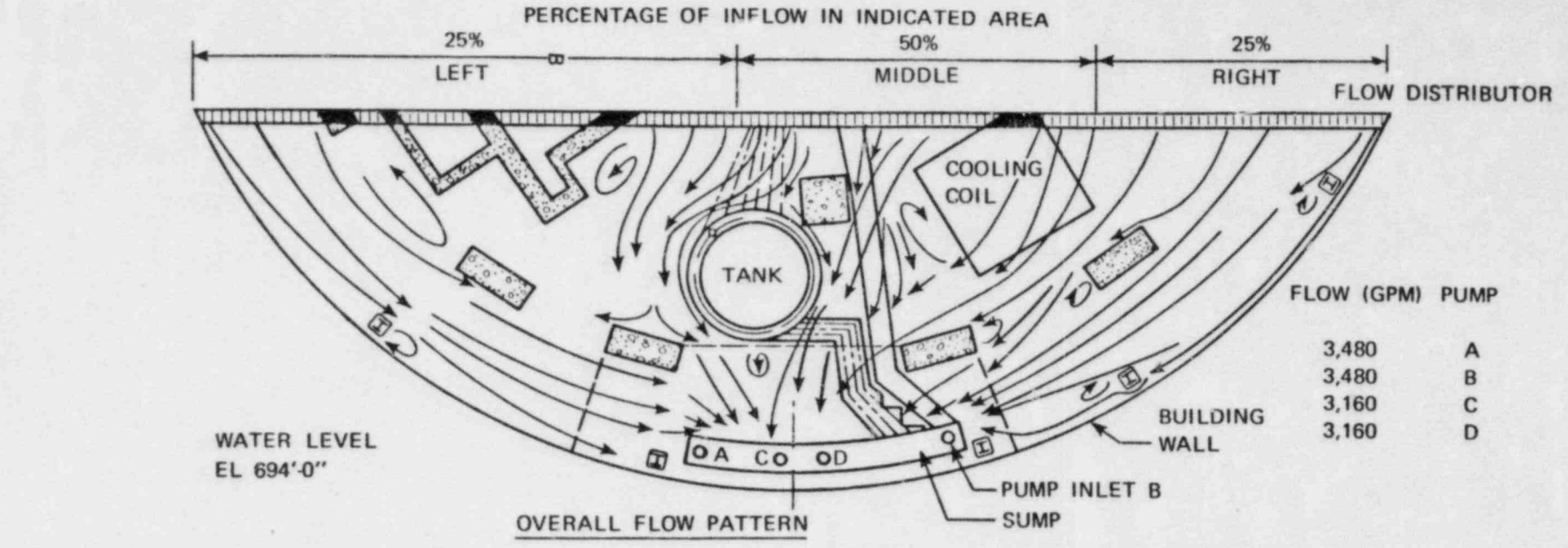

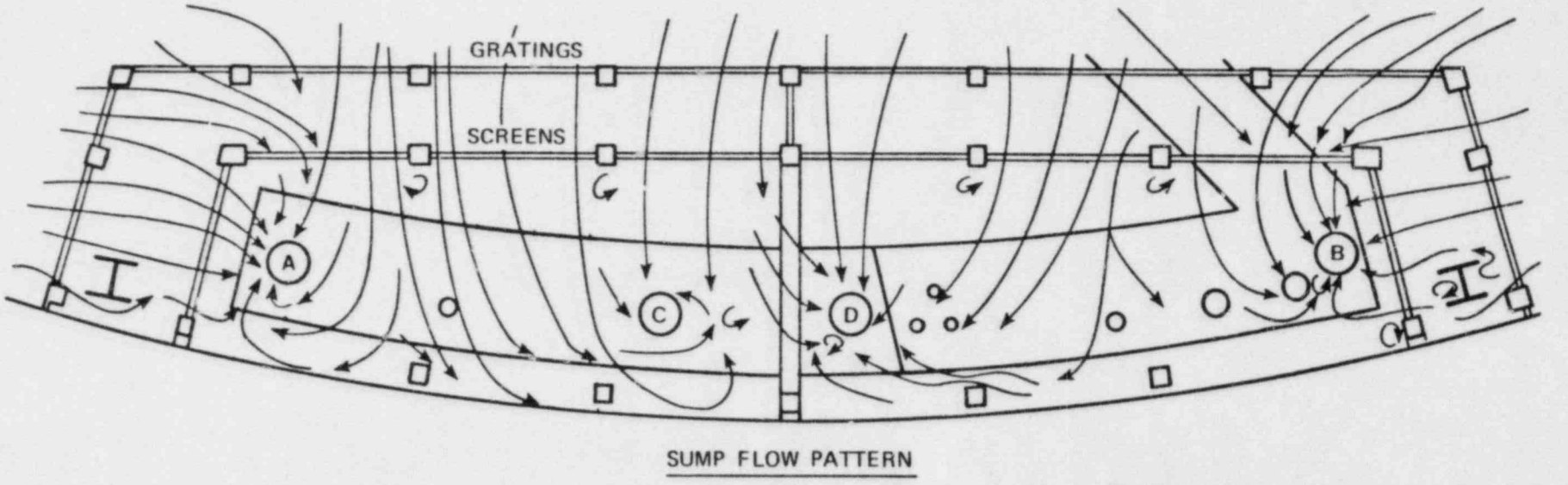

FIGURE 13 FLOW PATTERN WITH ALL PUMPS OPERATING
DISTRIBUTION 2

ARL

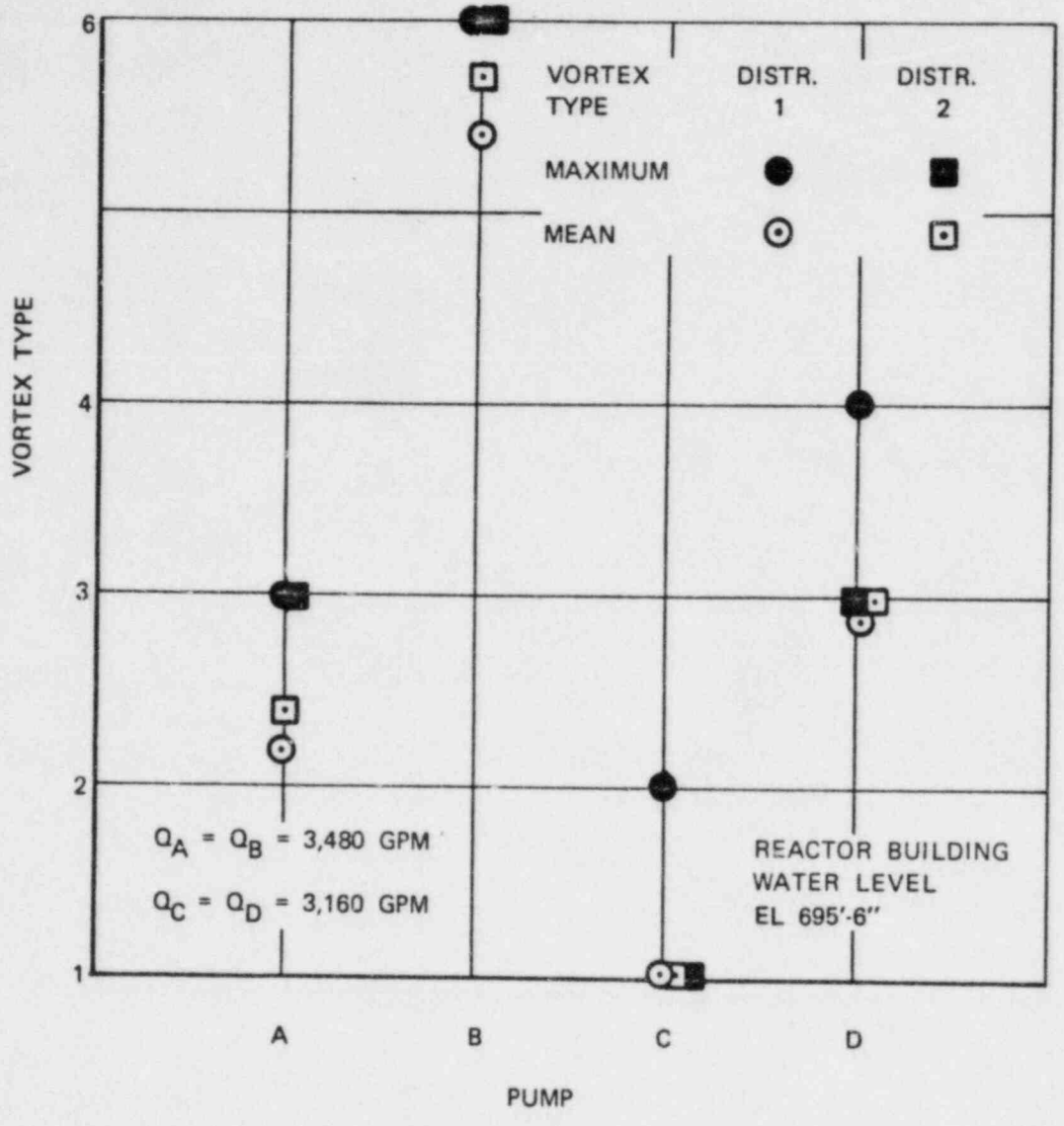

FIGURE 14 EFFECT OF FARFIELD FLOW DISTRIBUTION ON VORTEX SEVERITY WITH ORIGINAL DESIGN

ARL

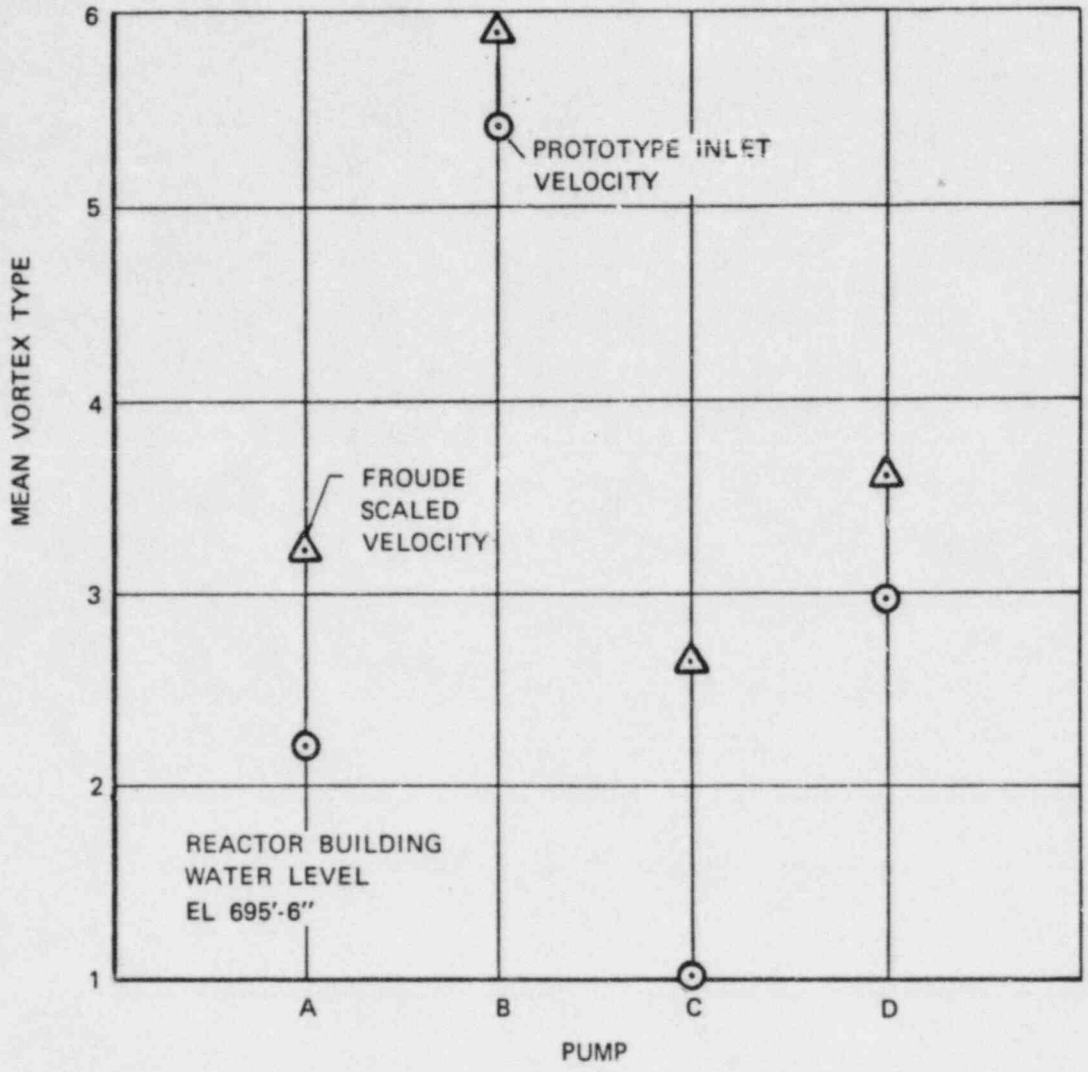

PUMP	FROUDE SCALED Q GPM	SCALED FLOW WITH PROTOTYPE INLET VELOCITY
A	3,480	6,029
B	3,480	6,029
C	3,160	5,474
D	3,160	5,474

FIGURE 15 EFFECT OF PUMP FLOWRATE ON VORTEX SEVERITY, ORIGINAL DESIGN

ARL

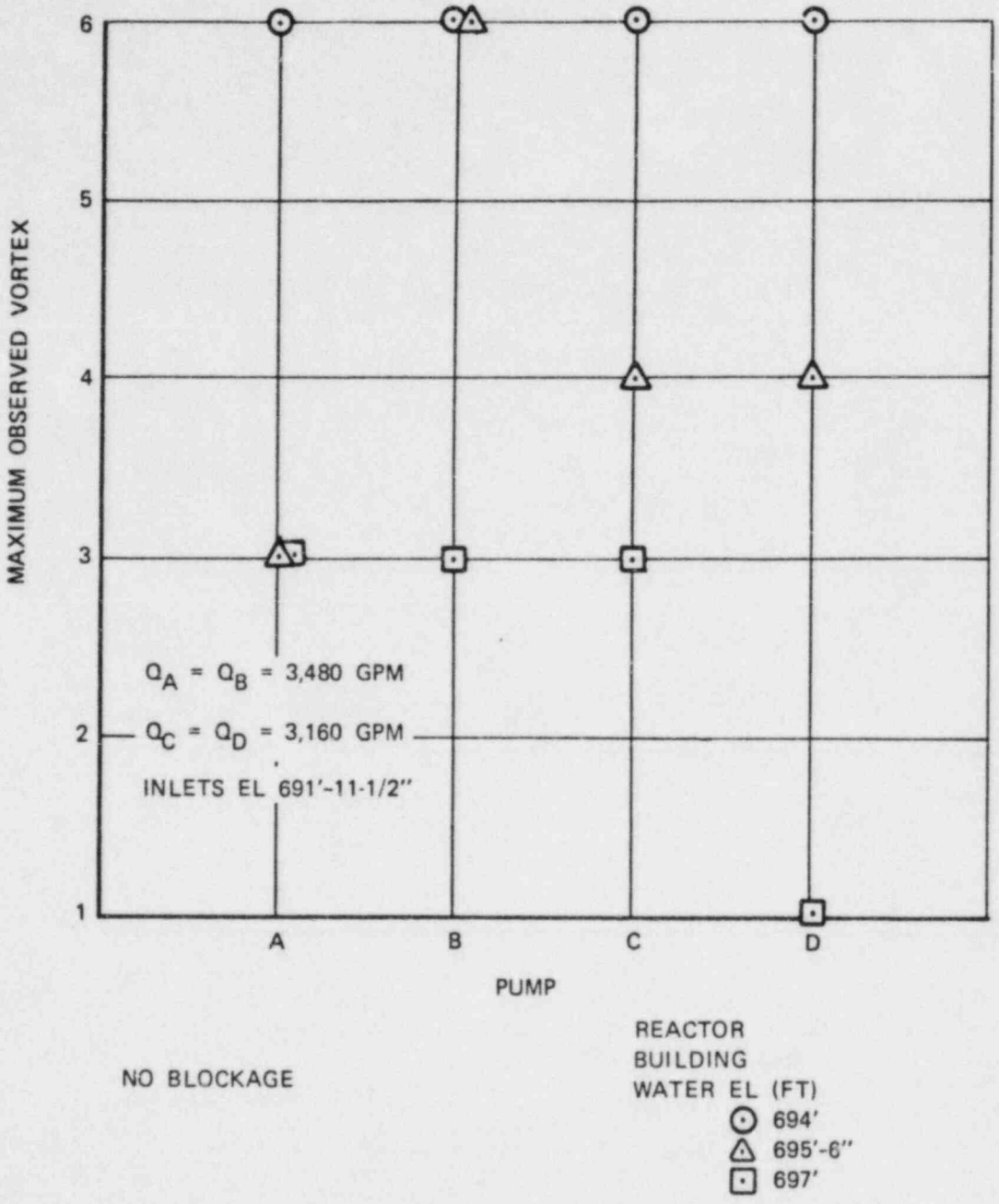

FIGURE 16 EFFECT OF WATER LEVEL ON MAXIMUM OBSERVED VORTICES, ORIGINAL DESIGN

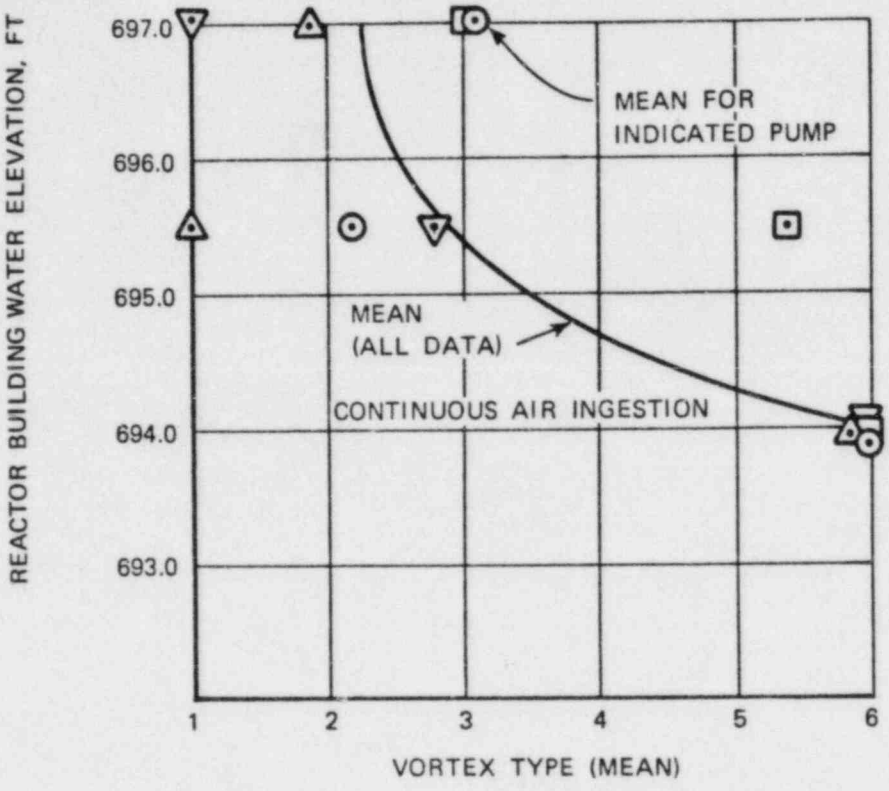

PUMP	SYMBOL	FLOW (GPM)
A	⊙	3,480
B	⊡	3,480
C	△	3,160
D	▽	3,160

NOTE:
NO GRATING OR SCREEN BLOCKAGE

FIGURE 17 VORTEX SEVERITY WITH ORIGINAL DESIGN

ARL

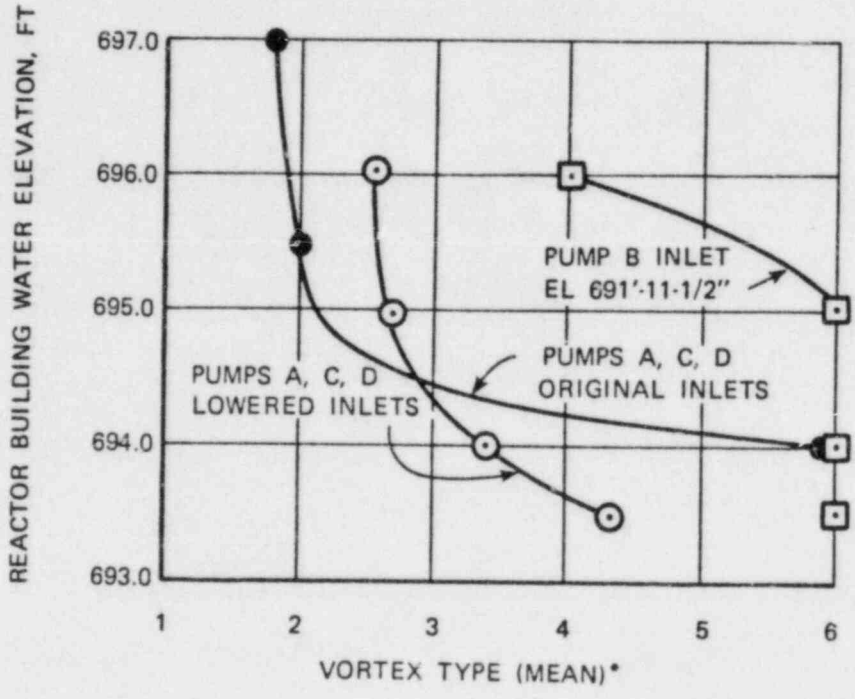

* AVERAGED OVER TIME FOR INDICATED INLETS

$Q_A = Q_B = 3{,}480$ GPM $\qquad Q_C = Q_D = 3{,}160$ GPM

NOTES:
1. NO RACK OR SCREEN BLOCKAGE
2. NO HORIZONTAL GRATING OVER INLETS

FIGURE 18 EFFECT OF LOWERED INLETS ON MEAN VORTEX SEVERITY

ARL

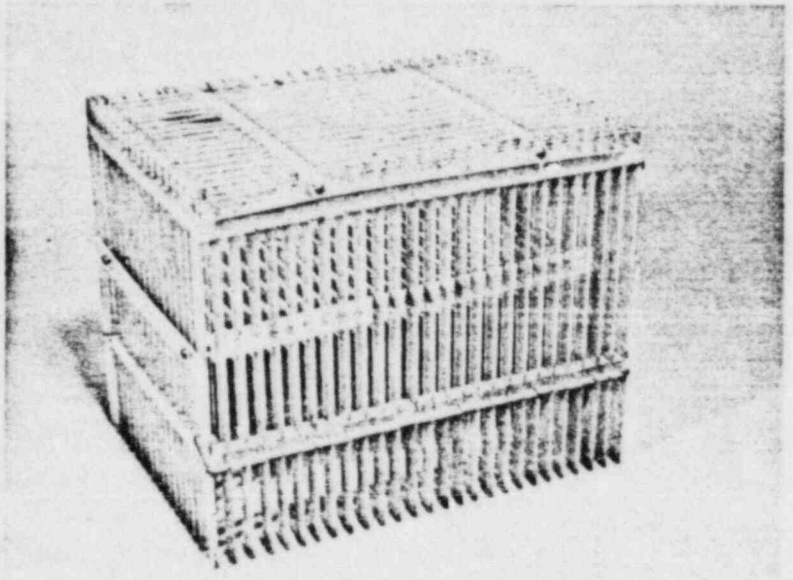

FIGURE 20 GRATING CAGE

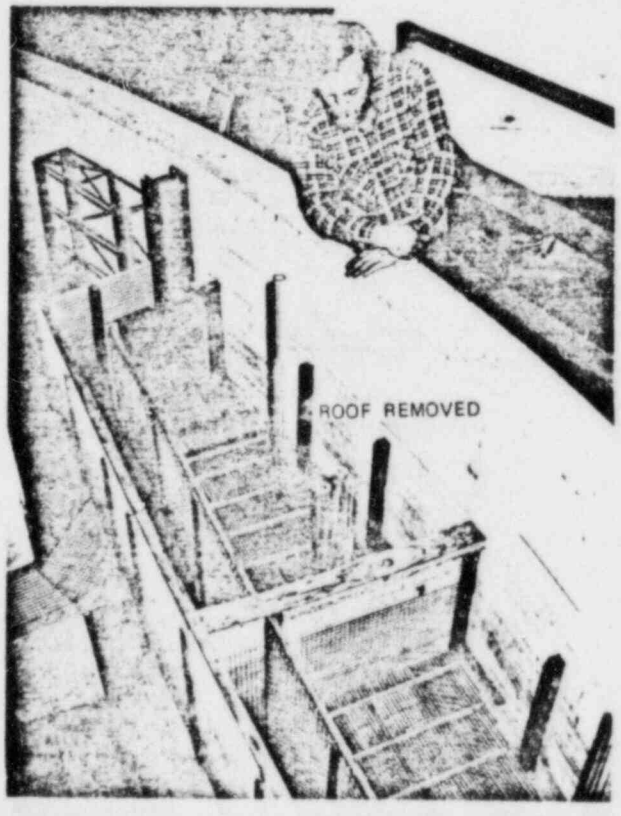

FIGURE 21 GRATINGS OVER INLETS

ARL

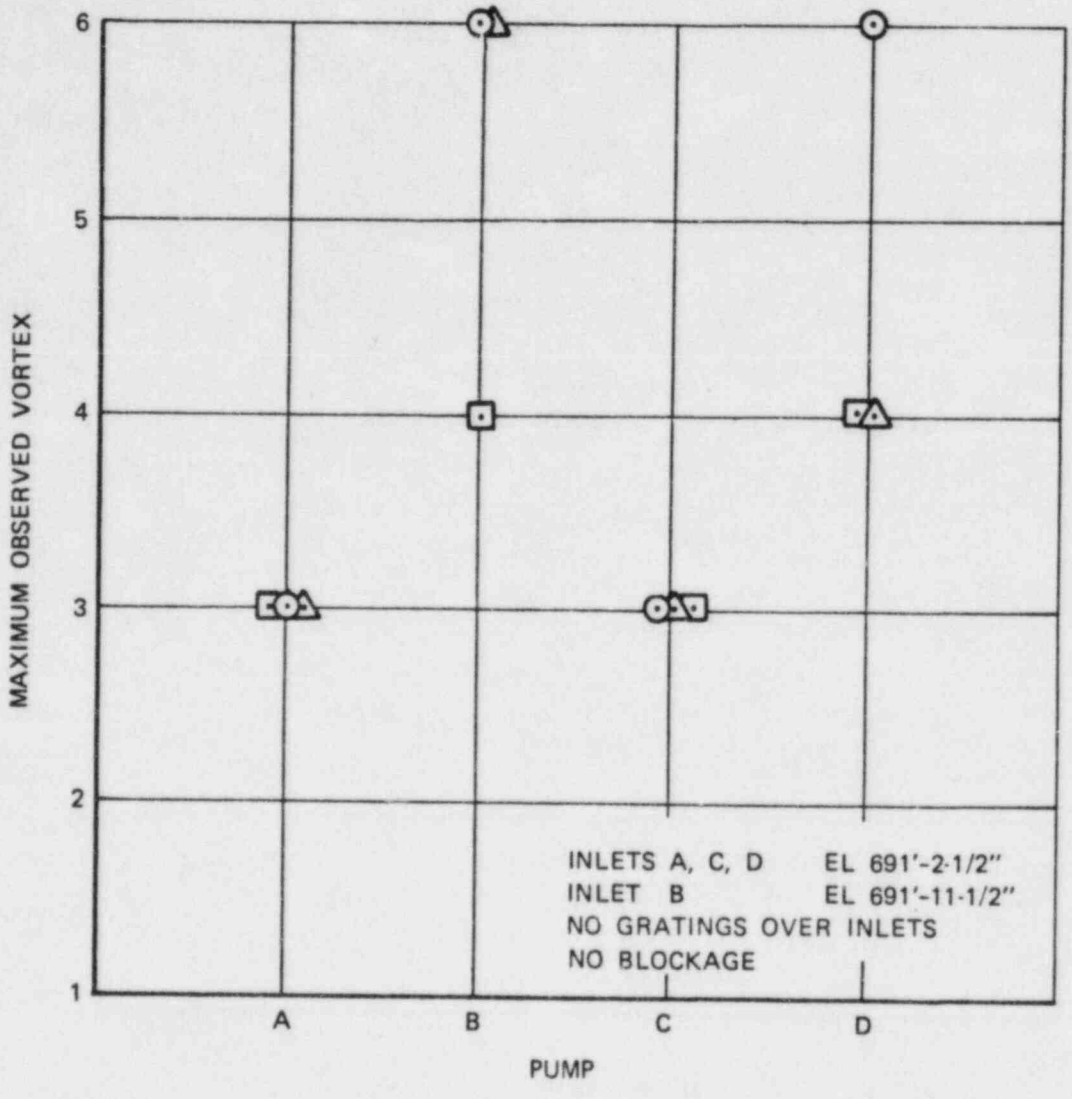

FIGURE 19 EFFECT OF WATER LEVEL ON MAXIMUM OBSERVED VORTICES WITH LOWERED INLETS

ARL

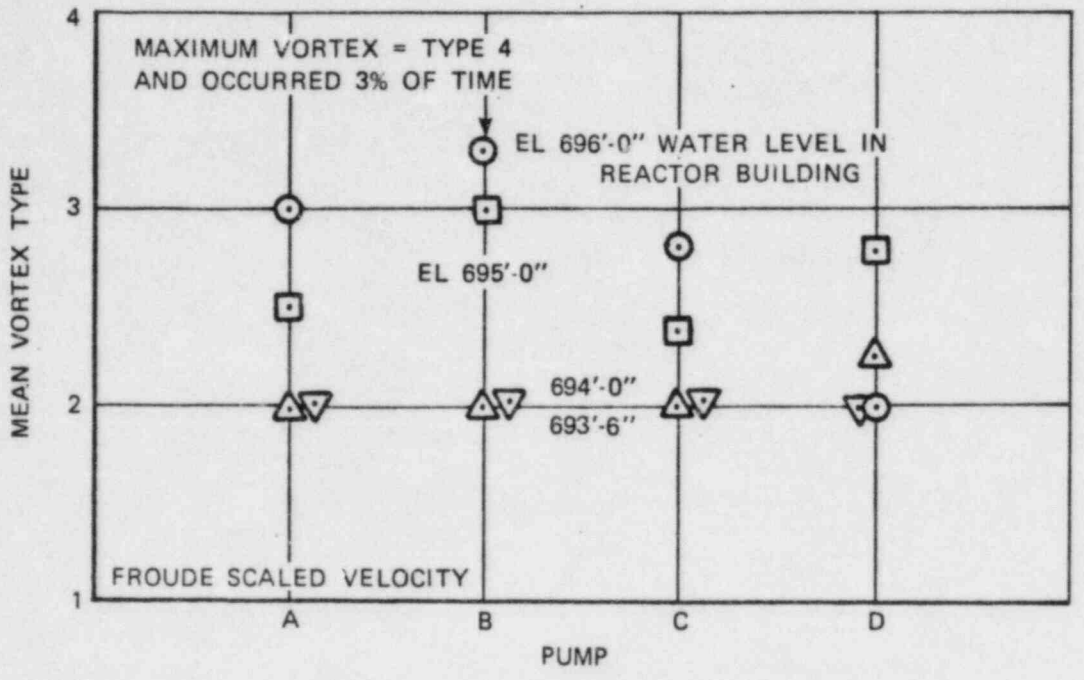

NOTES:
1. NO BLOCKAGE
2. INLETS A, C, D, EL 691'-2-1/2" (691.23')
   INLET B, EL 691'-11-1/2" (691.96')

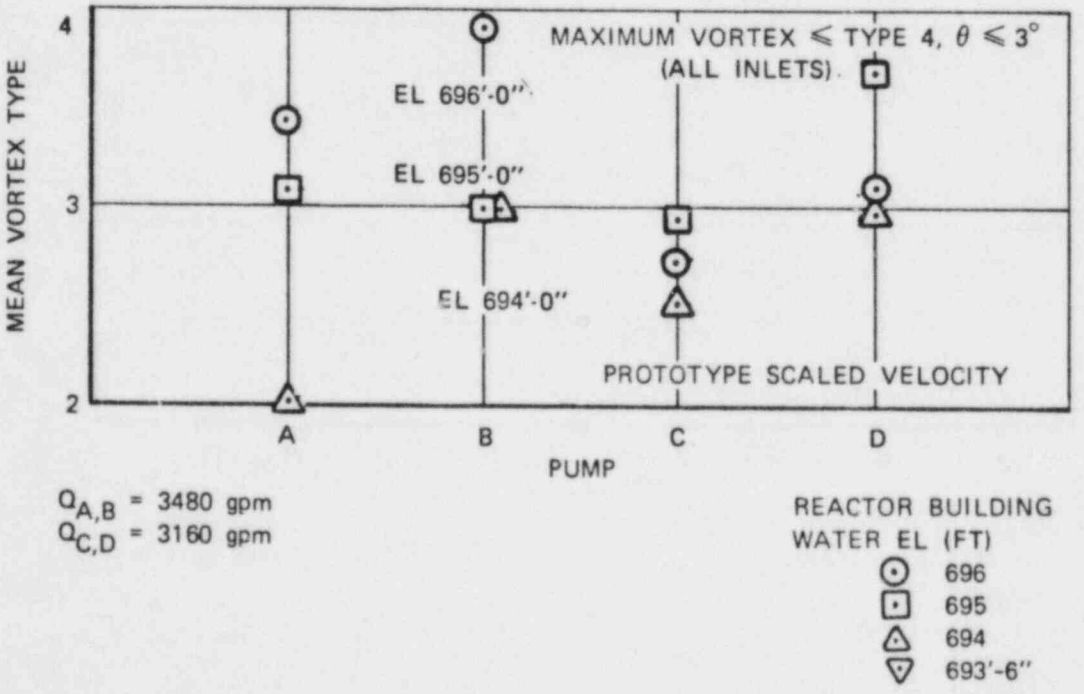

$Q_{A,B}$ = 3480 gpm
$Q_{C,D}$ = 3160 gpm

REACTOR BUILDING
WATER EL (FT)
696
695
694
693'-6"

FIGURE 22 VORTEX ACTIVITY WITH TWO LEVELS OF GRATING OVER SUMP

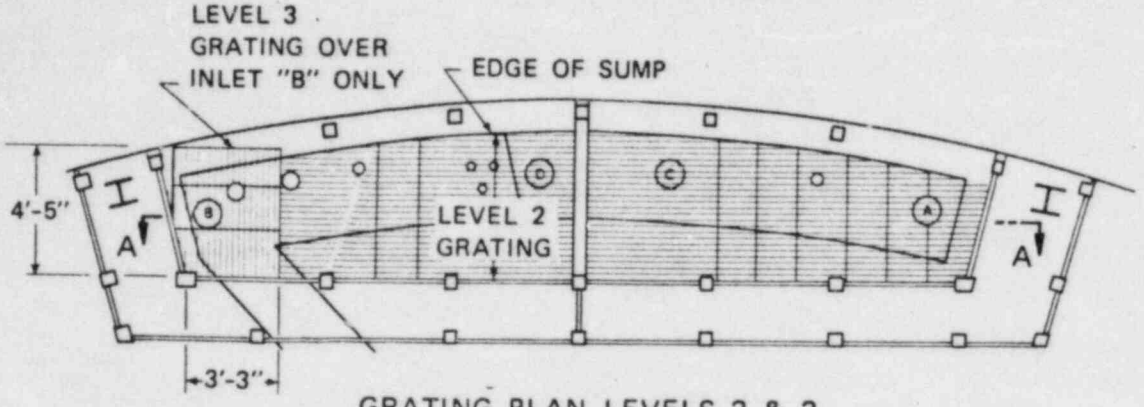

GRATING PLAN LEVELS 2 & 3

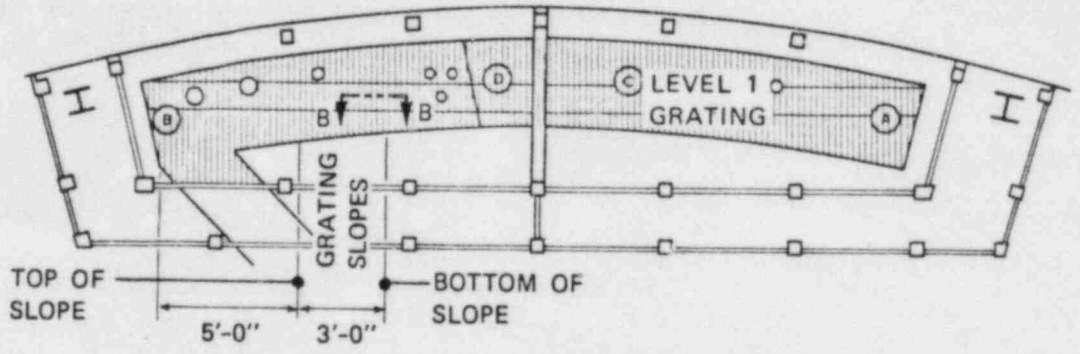

GRATING PLAN LEVEL 1

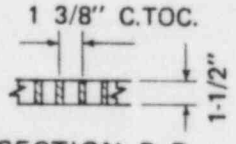

SECTION B-B

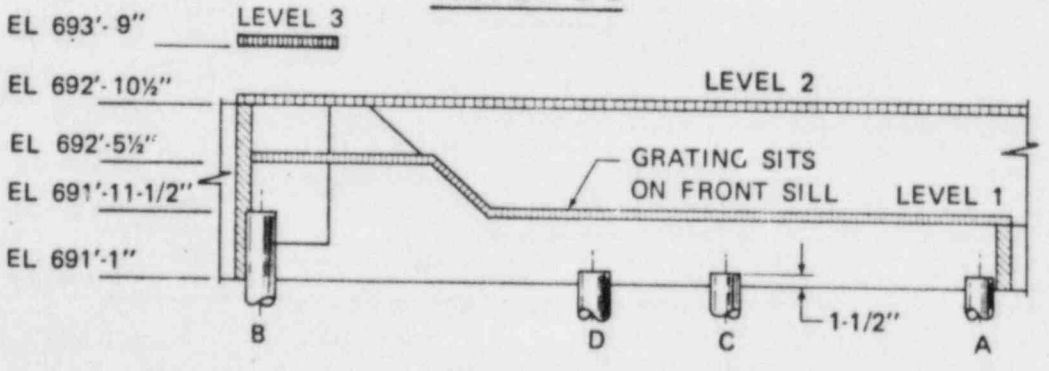

SECTION A-A

NO SCALE

FIGURE 23 DETAILS OF GRATINGS AND INLETS, MODIFIED DESIGN

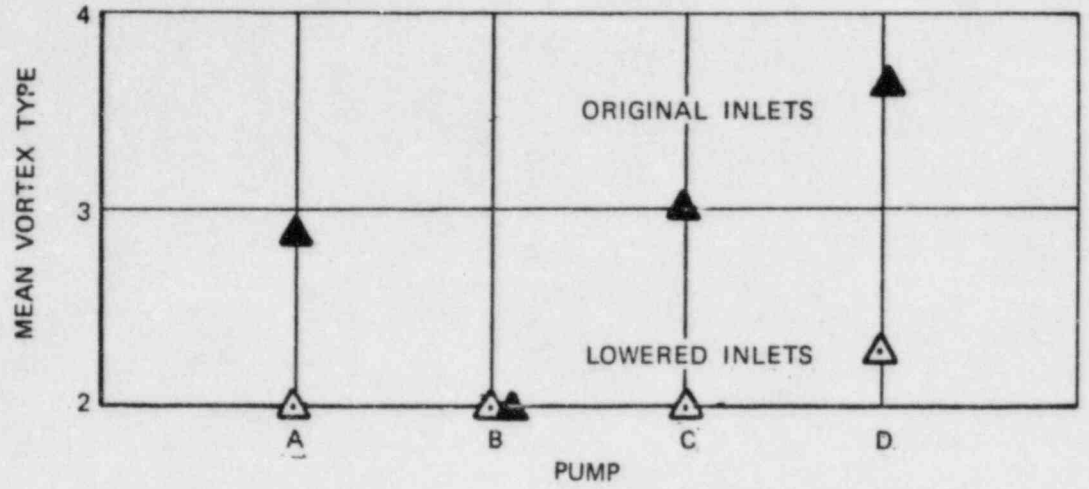

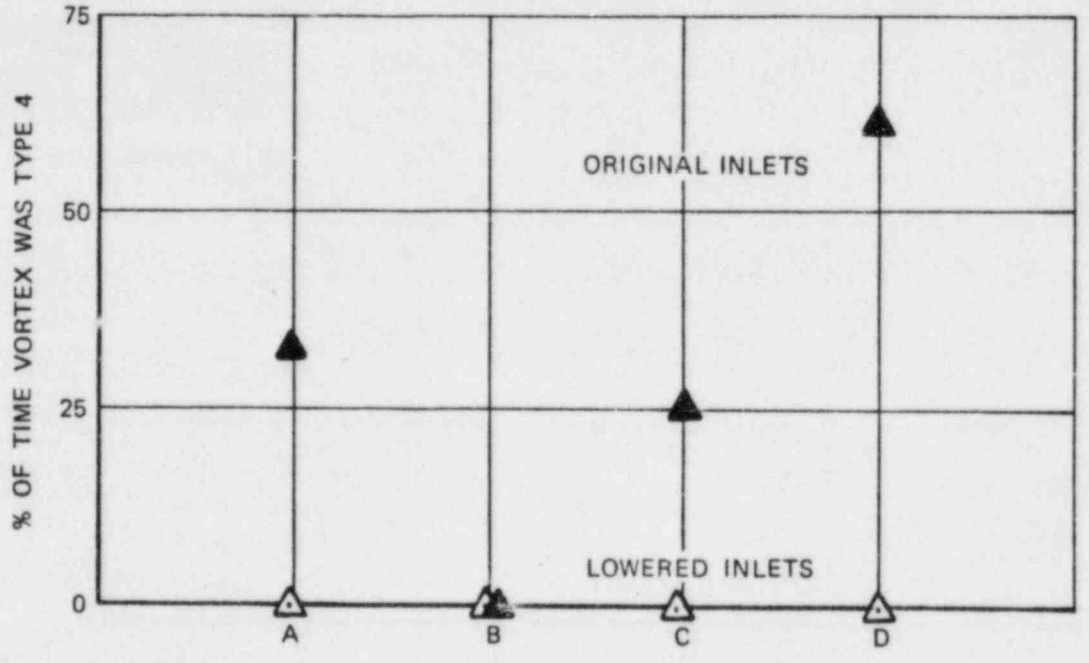

ORIGINAL INLETS

▲ ALL INLETS EL 691'-11-1/2"
INLETS A, C, D 2 LEVELS OF GRATINGS;
INLET B, 3 LEVELS

LOWERED INLETS

△ INLETS A, C, D, EL 691'-2-1/2"
INLET D, EL 691'-11-1/2"
2 LEVELS OF GRATINGS OVER INLETS

FROUDE SCALE VELOCITY

NO BLOCKAGE

FIGURE 24 EFFECT OF LOWERING INLETS ON VORTEX ACTIVITY AT LOW WATER LEVEL, REACTOR BUILDING WATER LEVEL EL 694'

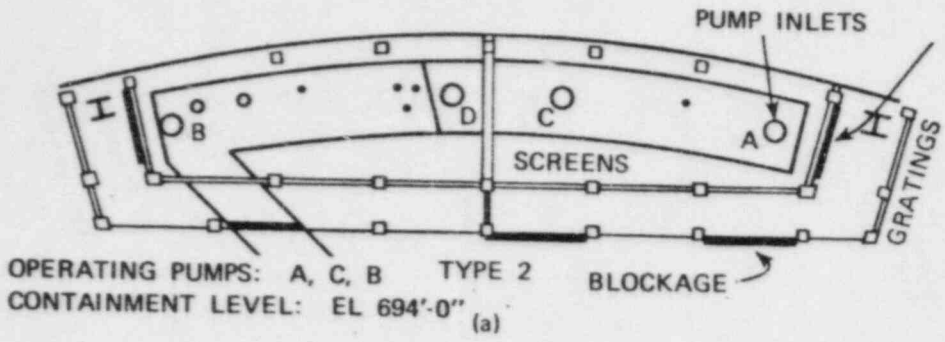

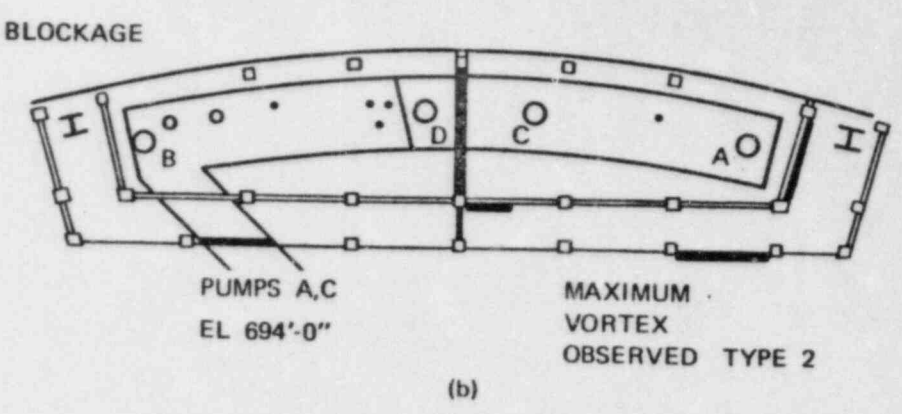

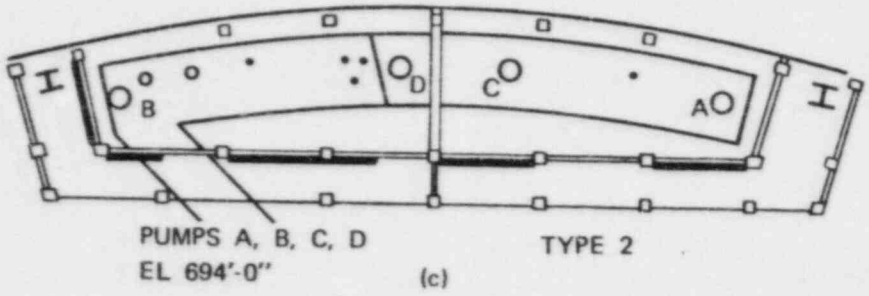

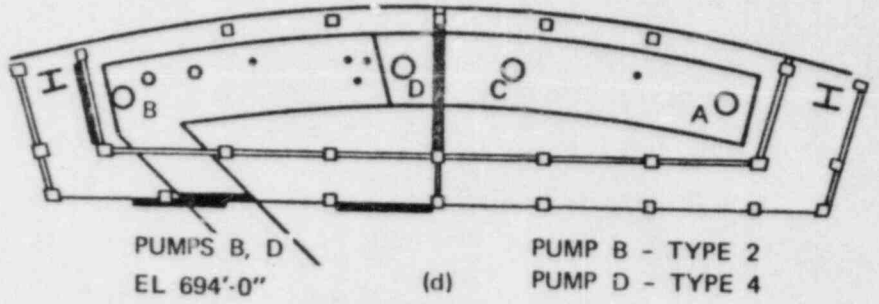

*PERSONNEL BARRIERS BLOCKED FROM COLUMNS TO WALL (FIGURE 1)

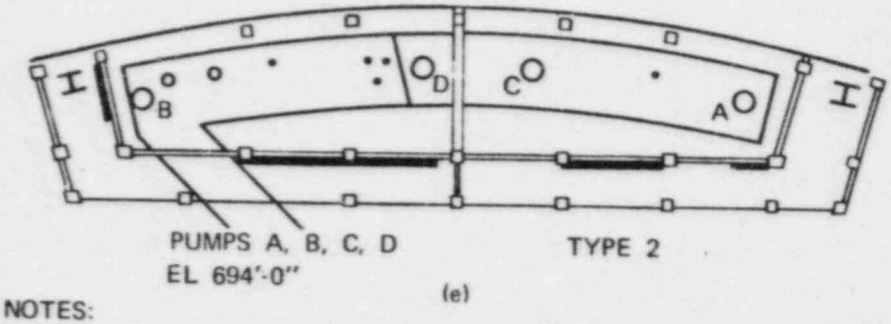

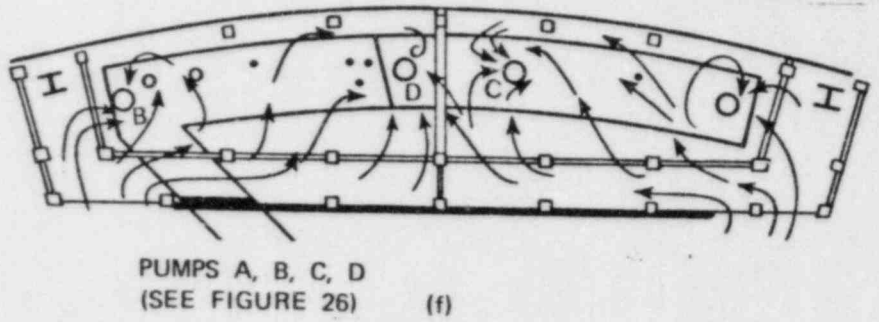

NOTES:

1. TRENCH BLOCKED ALL CASED: GRATINGS AS SHOWN IN FIGURE 23
2. $Q_A = Q_B = 3480$ GPM
   $Q_C = Q_D = 3160$ GPM
3. "AFTER SWITCH OVER FLOWS"

FIGURE 25 TYPICAL BLOCKAGES

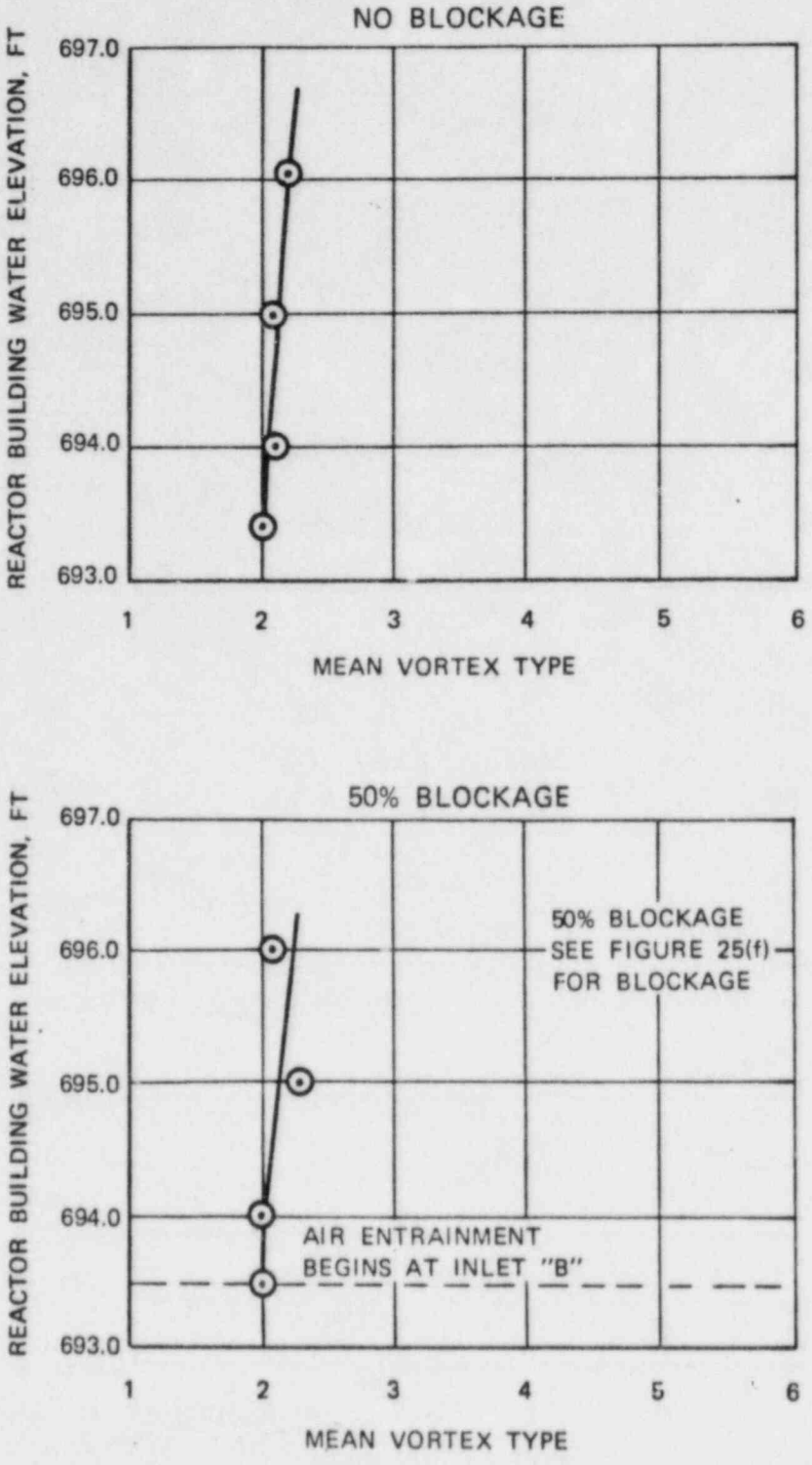

1. FROUDE SCALED FLOW
2. INLETS A, C, D, EL 691'-2-1/2" WITH TWO LEVELS OF GRATINGS (FIGURE 23)
3. INLET B, EL 691'-11-1/2" WITH THREE LEVELS OF GRATINGS
4. "AFTER SWITCH OVER FLOWS", $Q_{A,B}$ = 3480 gpm AND $Q_{C,D}$ = 3160 gpm

FIGURE 26 MEAN VORTEX SEVERITY WITH MULTIPLE LEVELS OF GRATINGS MODIFIED DESIGN

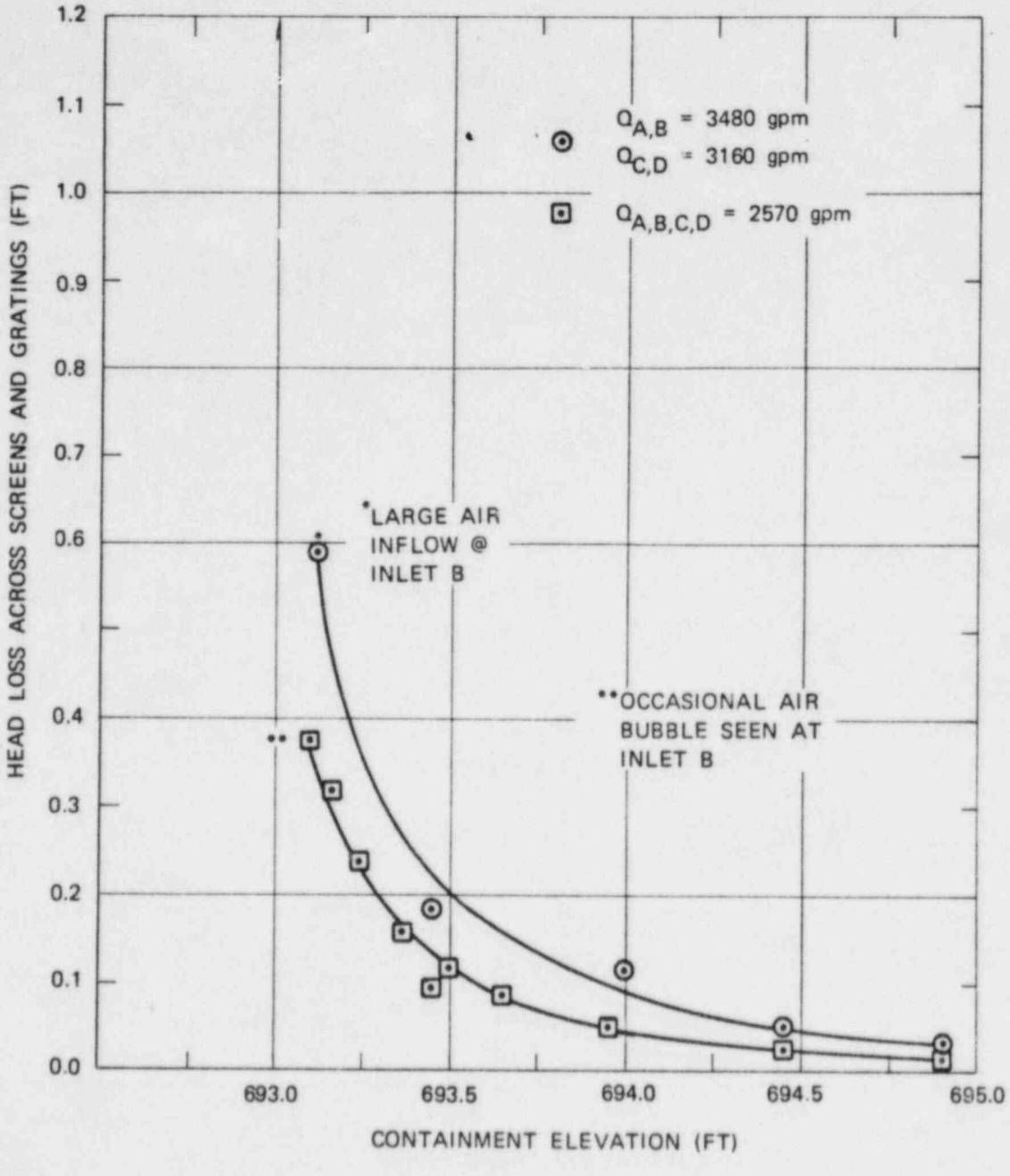

NOTE: FOR GRATING AND INLET DETAILS SEE FIGURE 23

FIGURE 27 HEAD LOSS WITH FOUR PUMP OPERATION AND NO BLOCKAGE, MODIFIED DESIGN

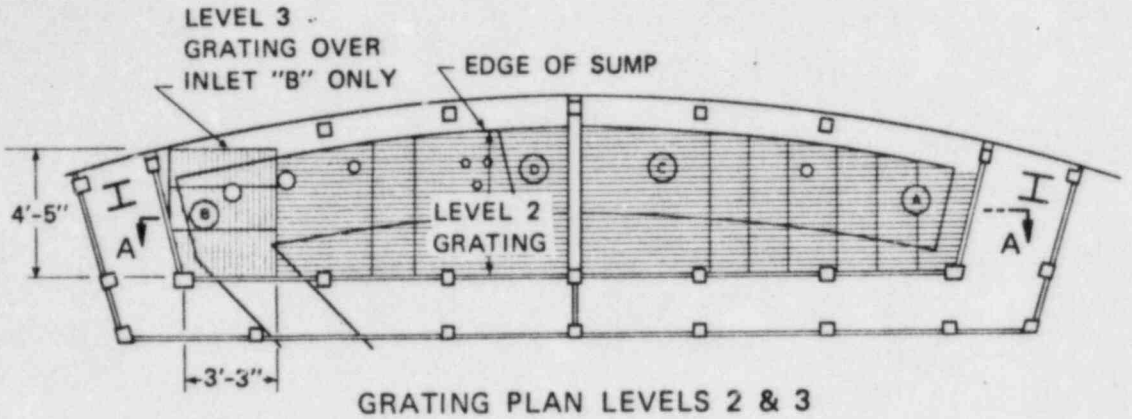

GRATING PLAN LEVELS 2 & 3

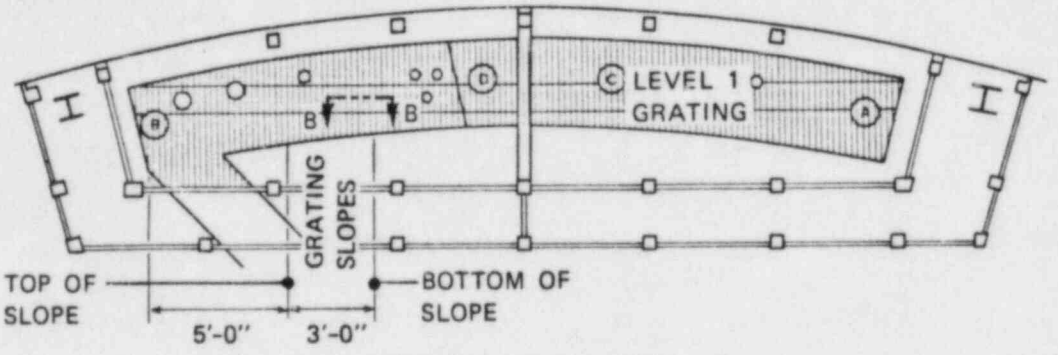

GRATING PLAN LEVEL 1

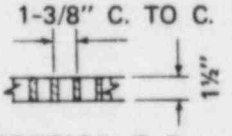

SECTION B-B

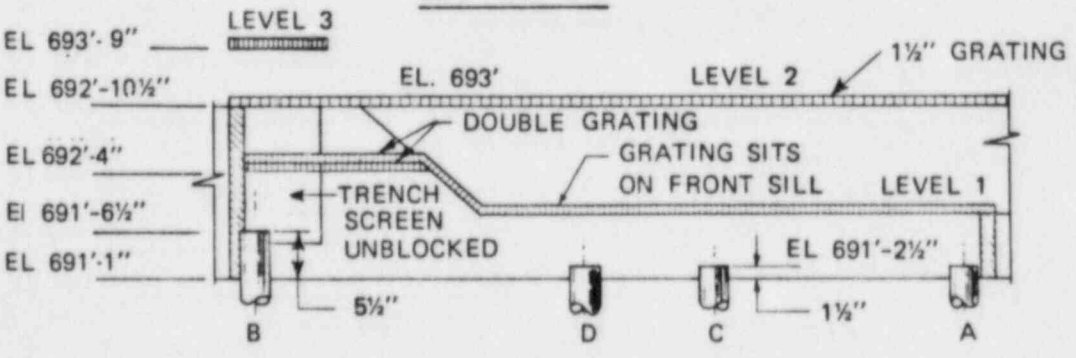

SECTION A-A

NO SCALE

FIGURE 28 FINAL DESIGN, INLET AND GRATING DETAILS

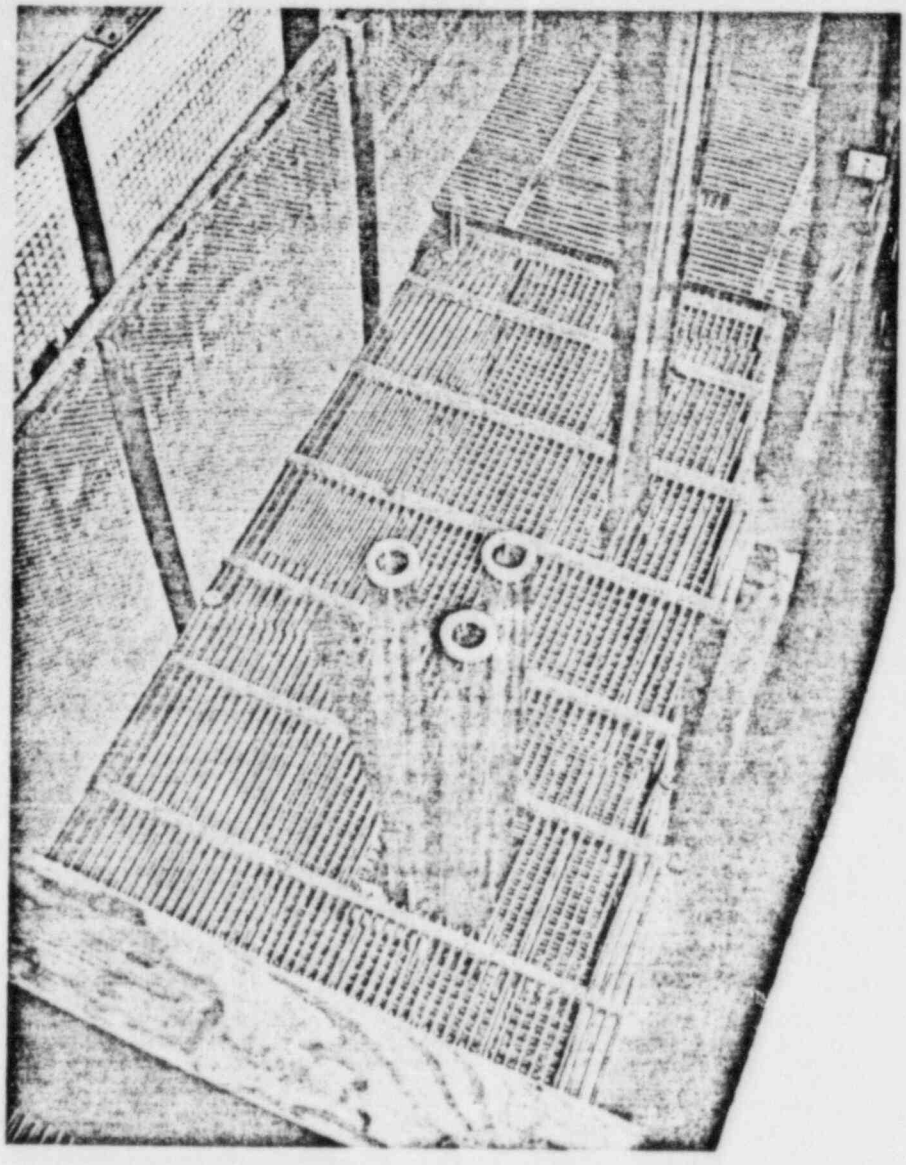

FIGURE 29 FINAL GRATINGS OVER INLETS B AND D

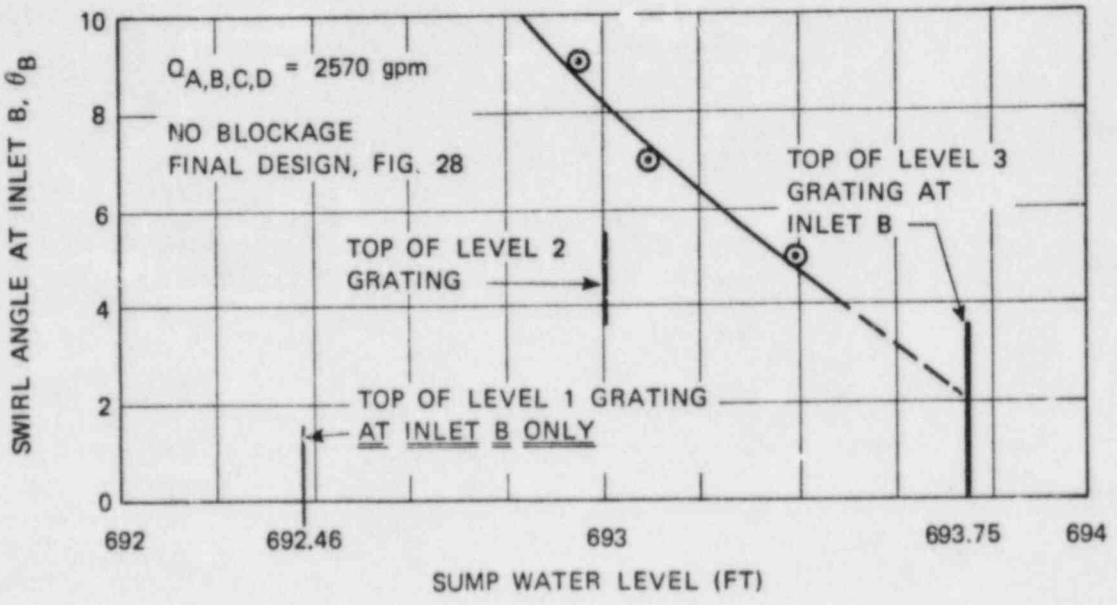

FIGURE 30 EFFECT OF SUMP WATER LEVEL ON INLET B SWIRL ANGLE

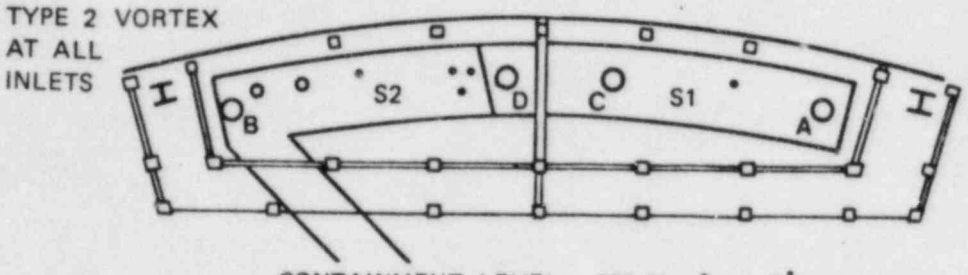

CONTAINMENT LEVEL = 693.2′ $\theta_B = 9^\circ$
S1 = 692.9′
S2 = 692.9′

(a) NO BLOCKAGE

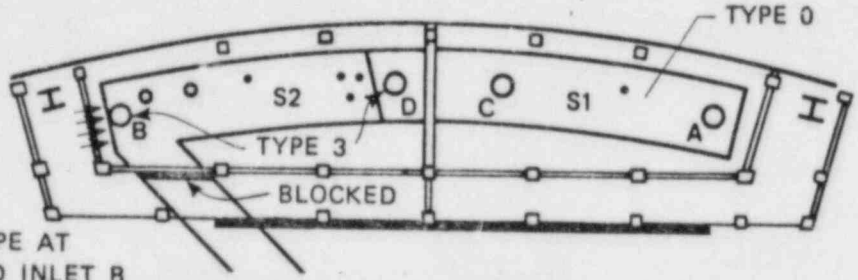

NOTE 1:
ONSET, NAPPE AT
SCREEN AND INLET B
ENTRAINS OCCASIONAL
AIR BUBBLE

CONTAINMENT LEVEL = 693.6′ $\theta_B = 4^\circ$ $\theta_C = 8^\circ\text{-}10^\circ$
S1 = 692.9′
S2 = 692.9′

(b) WORST RACK BLOCKAGE

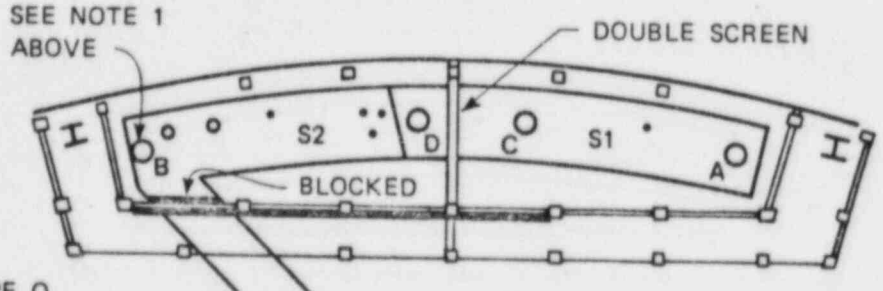

TYPE O
VORTICES AT
INLETS A, C, D

CONTAINMENT LEVEL = 693.8′
S1 = 693.5′
S2 = 693.1′

(c) WORST SCREEN BLOCKAGE

FIGURE 31 MINIMUM ACCEPTABLE CONTAINMENT LEVELS WITH FOUR PUMP OPERATION, INLET FLOW 2,570 GPM/PUMP, FINAL DESIGN

ARL

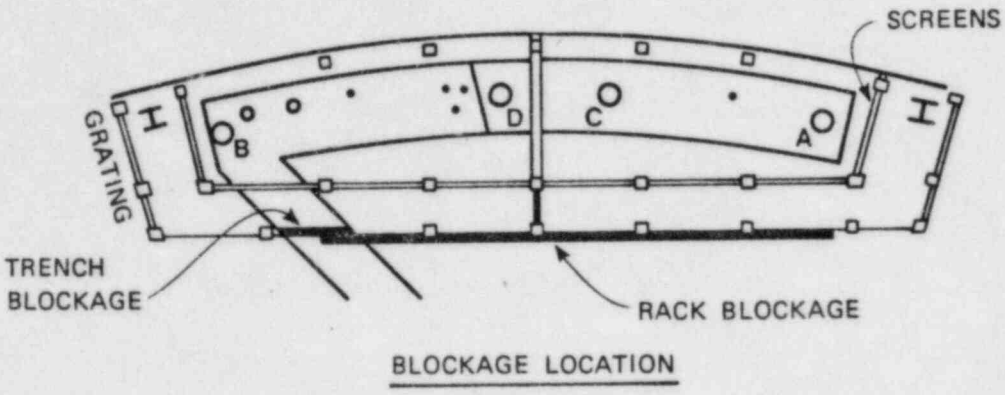

BLOCKAGE LOCATION

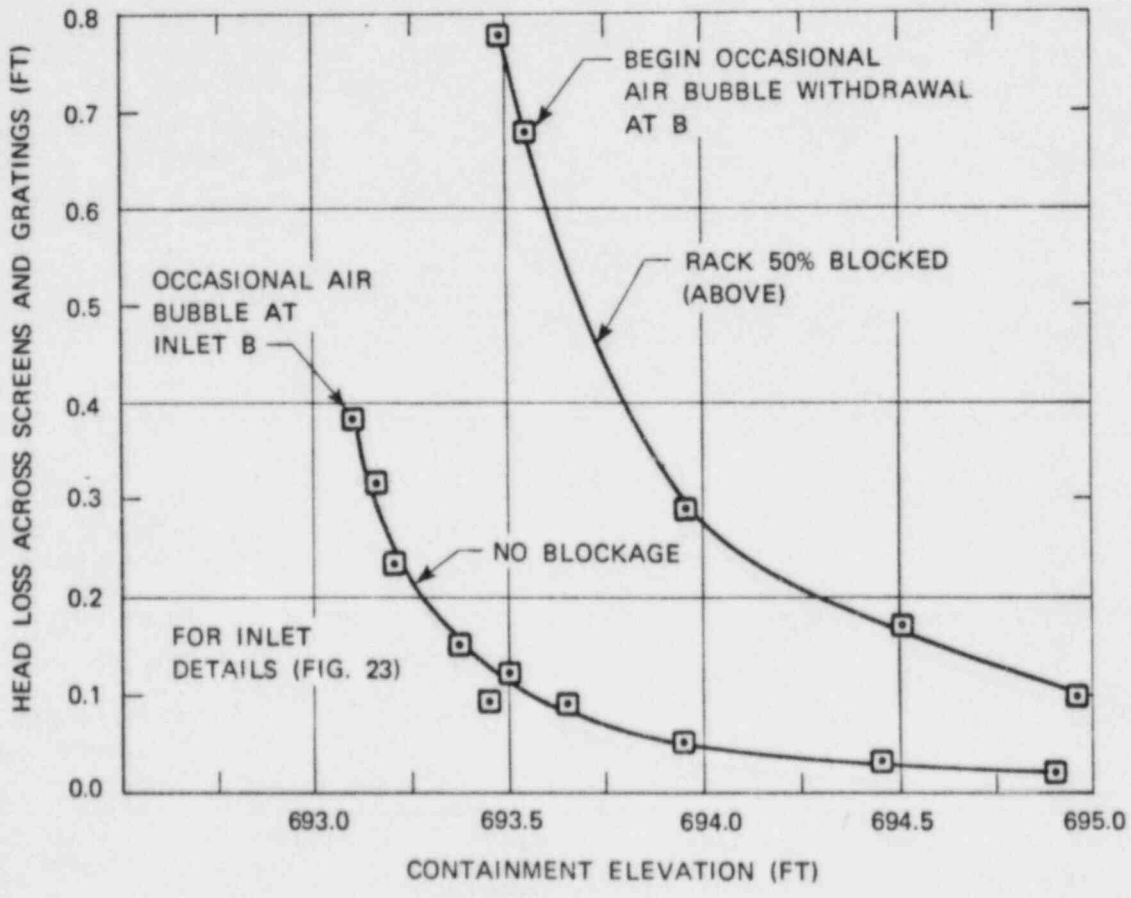

NOTE: TRENCH BLOCKED FOR ALL ABOVE DATA

FIGURE 32 AFFECT OF WORST RACK BLOCKAGE ON HEAD LOSS DURING FOUR PUMP OPERATION, INLET FLOW 2570 GPM, FINAL DESIGN

ARL

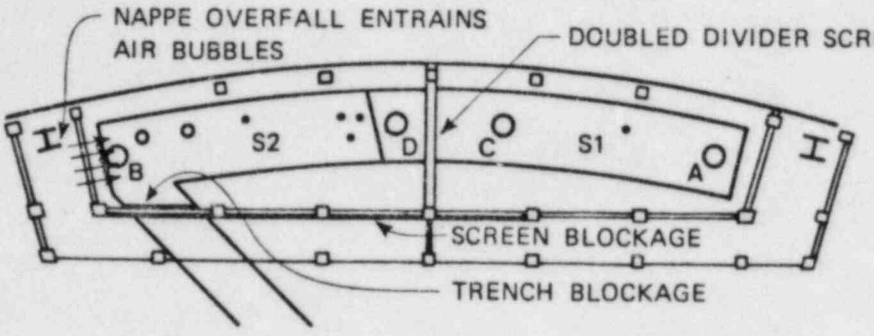

BLOCKAGE LOCATION

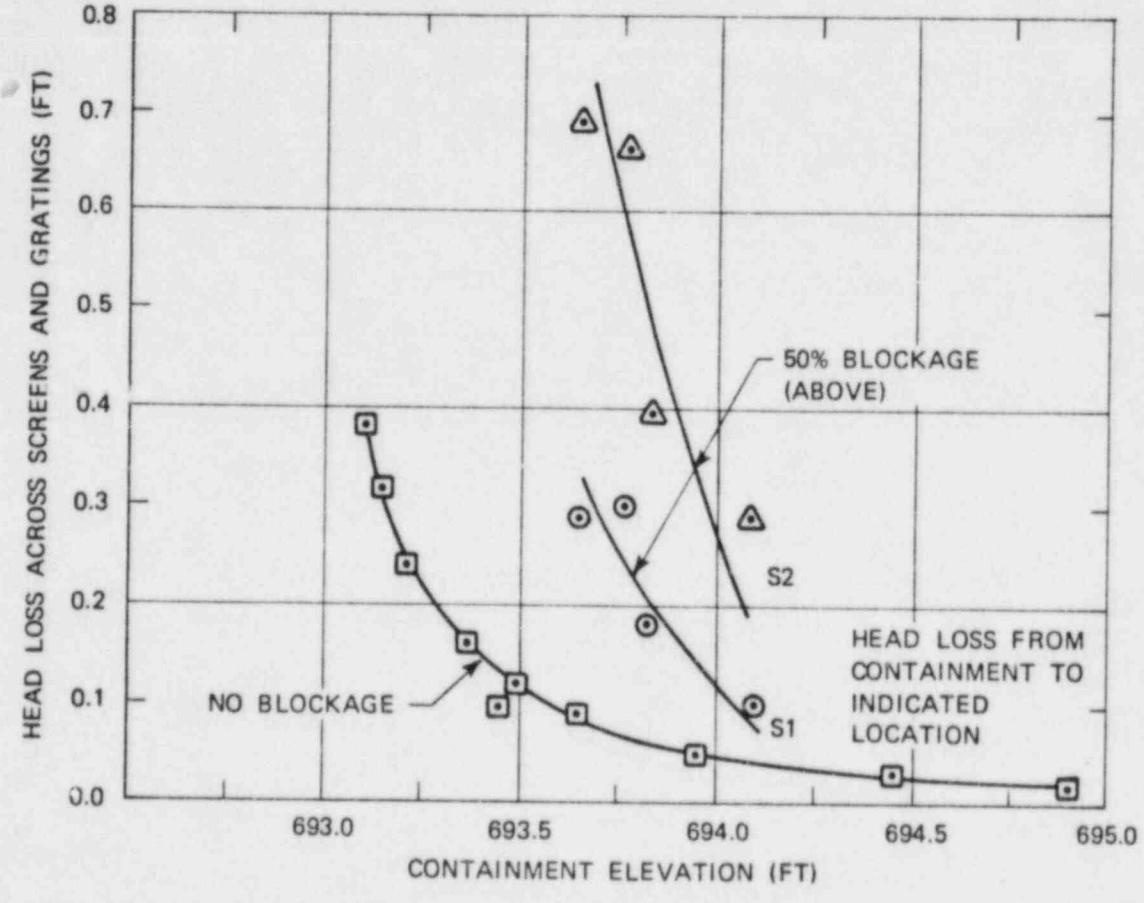

FIGURE 33 HEAD LOSS WITH WORST SCREEN BLOCKAGE DURING FOUR PUMP OPERATION, INLET FLOW 2570 GPM, FINAL DESIGN

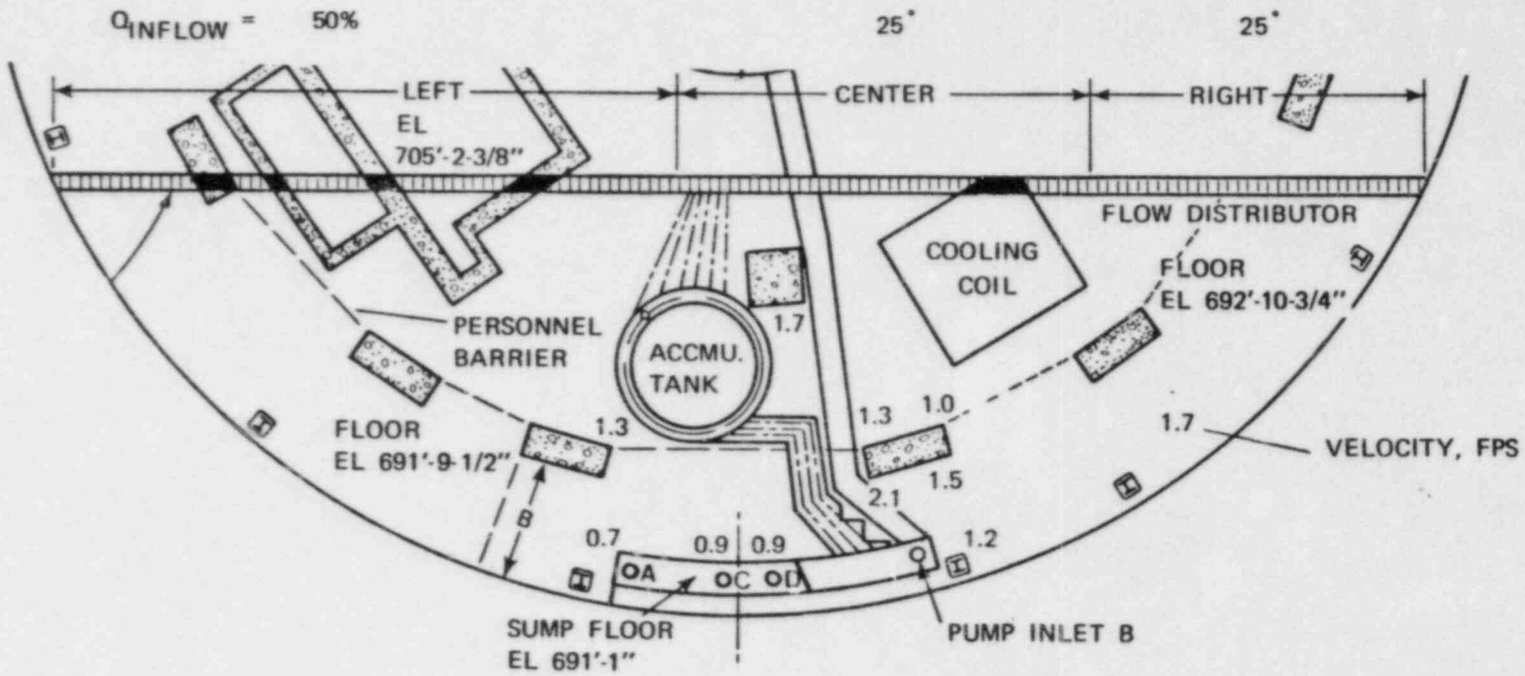

NOTE: NO AIR ENTRAINMENT
WITH CONTAINMENT
EL. 693.2'

TEST CONDITIONS:
1. FOUR PUMPS OPERATING
   $Q_{A,B,C,D}$ = 2,570 gpm
2. NO BLOCKAGE
3. INLETS A,C,D = EL. 691.21'
   INLET B EL. 691.54'

FIGURE 34 VELOCITIES ON CONTAINMENT FLOOR, CONTAINMENT WATER LEVEL EL 693.2 FT

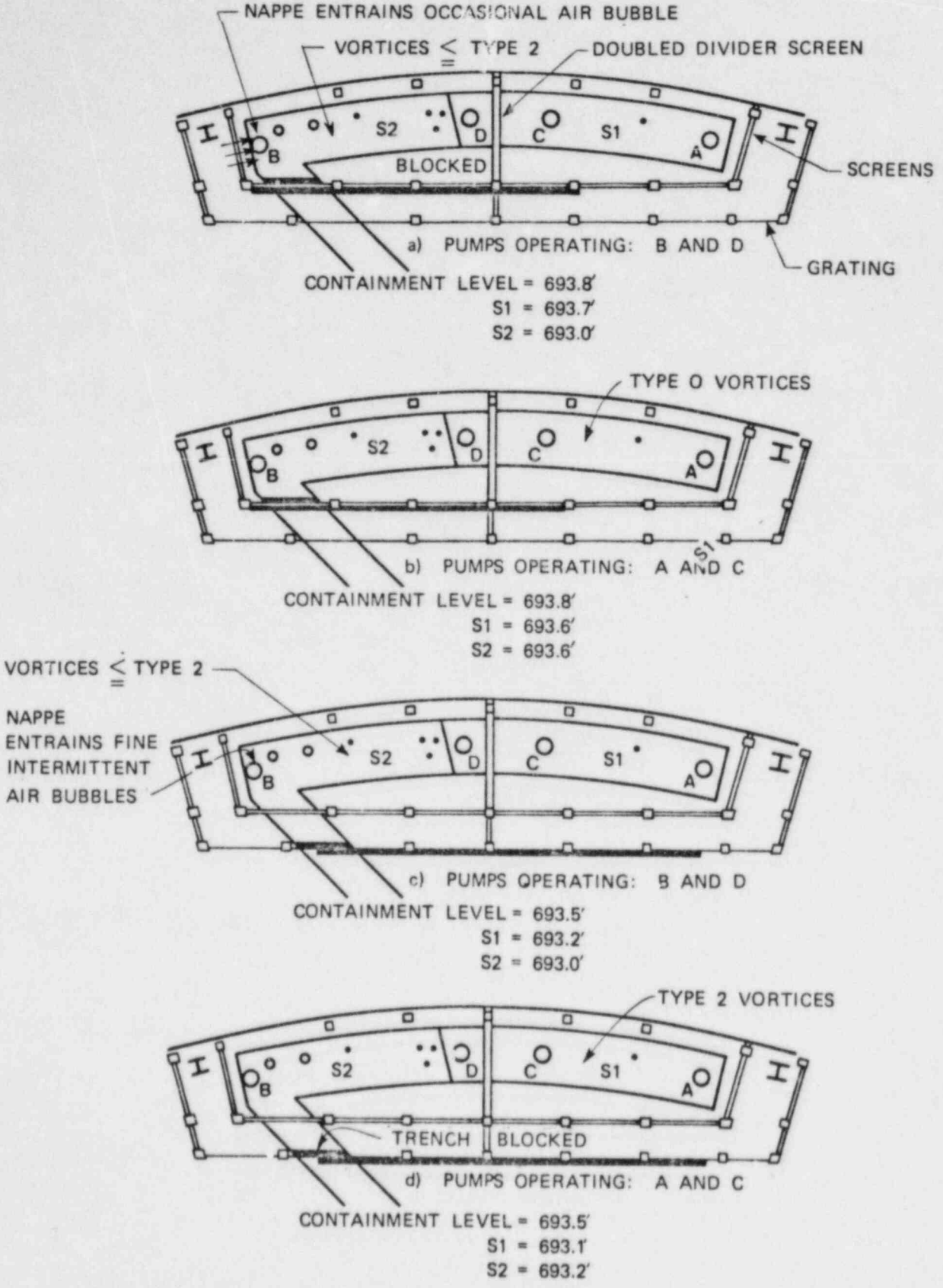

FIGURE 35 MINIMUM CONTAINMENT LEVELS WITH TWO PUMP OPERATION, INLET FLOW 3480 gpm, WORST BLOCKAGE CONDITIONS FINAL DESIGN

ARL

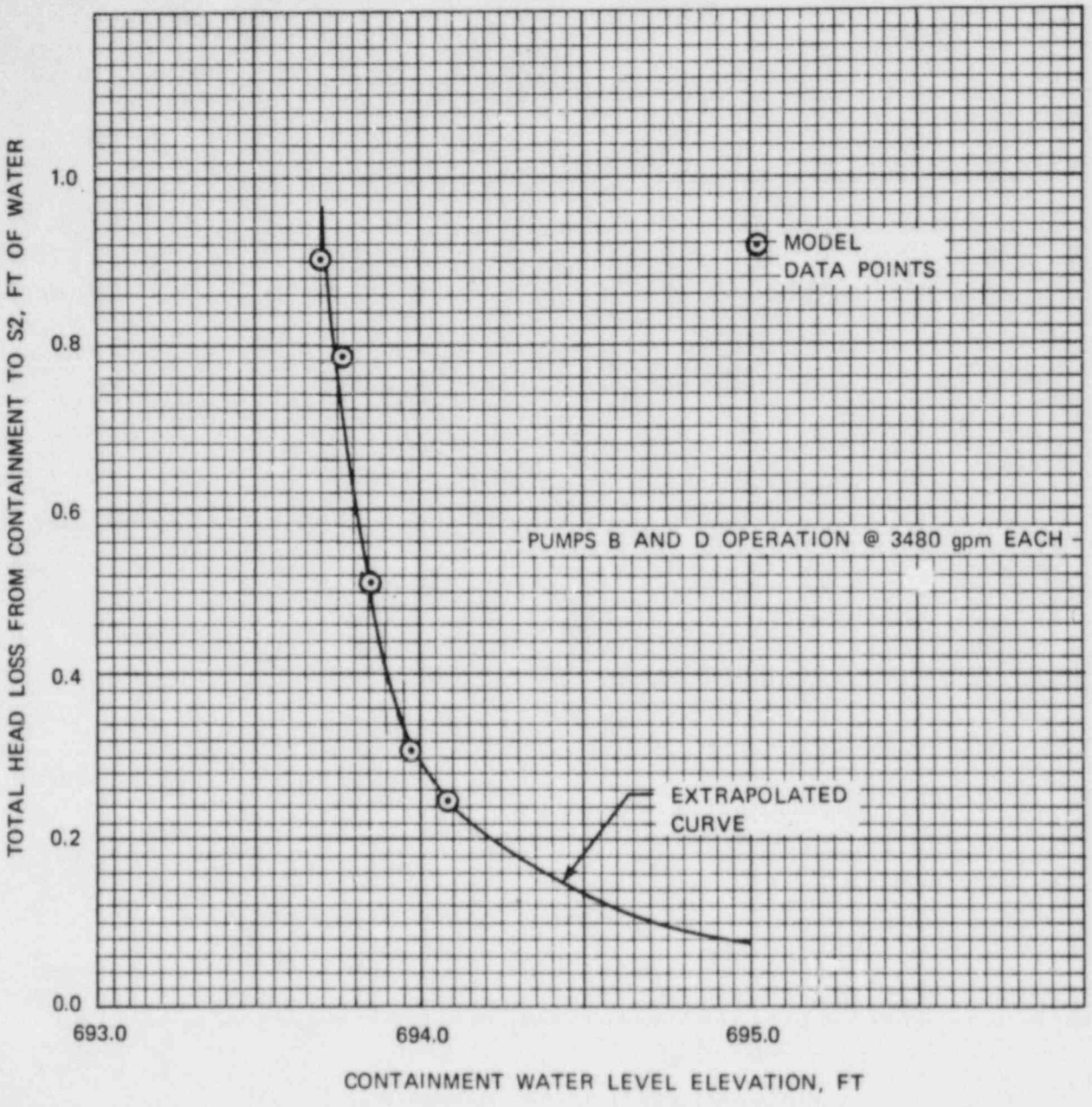

NOTE: SEE FIGURE 35(a) FOR BLOCKAGE

FIGURE 36 TOTAL HEAD LOSS FROM CONTAINMENT TO LOCATION S2 WITH WORST SCREEN BLOCKAGE CONDITION